AD-A042 999 ARMY ENGINEER WATERWAYS EXPERIMENT STATION VICKSBURG MISS F/G 15/4
ACQUISITION OF TERRAIN INFORMATION USING LANDSAT MULTISPECTRAL --ETC(U)
JUN 77 H STRUVE, W E GRABAU, H W WEST

UNCLASSIFIED WES-TR-M-77-2-1 NL

1 OF 1
AD A042999

END
DATE FILMED
9-77
DDC

TECHNICAL REPORT M-77-2

ACQUISITION OF TERRAIN INFORMATION USING LANDSAT MULTISPECTRAL DATA

Report I

CORRECTION OF LANDSAT MULTISPECTRAL DATA FOR EXTRINSIC EFFECTS

by

Horton Struve, Warren E. Grabau, Harold W. West

Mobility and Environmental Systems Laboratory
U. S. Army Engineer Waterways Experiment Station
P. O. Box 631, Vicksburg, Miss. 39180

June 1977
Report I of a Series

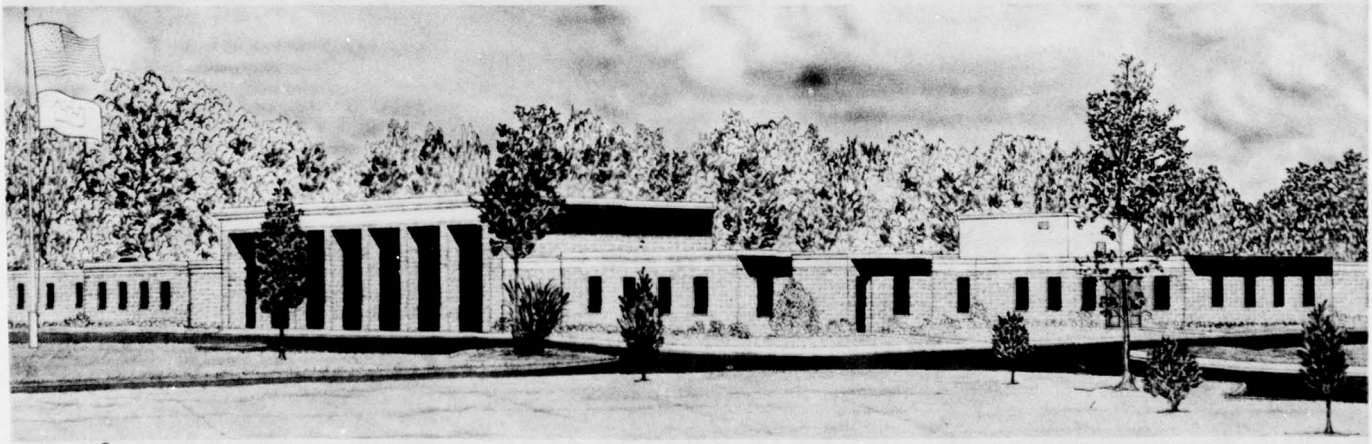

Prepared for Assistant Secretary of the Army (R&D)
Department of the Army
Washington, D. C. 20314

Under Project 4A061101A91D, Task 02
Work Unit 095 Q6

Destroy this report when no longer needed. Do not return
it to the originator.

Unclassified

SECURITY CLASSIFICATION OF THIS PAGE *(When Data Entered)*

REPORT DOCUMENTATION PAGE

READ INSTRUCTIONS BEFORE COMPLETING FORM

1. REPORT NUMBER: Technical Report M-77-2-1

2. GOVT ACCESSION NO.

3. RECIPIENT'S CATALOG NUMBER

4. TITLE *(and Subtitle)*: ACQUISITION OF TERRAIN INFORMATION USING LANDSAT MULTISPECTRAL DATA. Report 1, CORRECTION OF LANDSAT MULTISPECTRAL DATA FOR EXTRINSIC EFFECTS.

5. TYPE OF REPORT & PERIOD COVERED: Report 1 of a series

6. PERFORMING ORG. REPORT NUMBER

7. AUTHOR(s): Horton/Struve, Warren E./Grabau, Harold W./West

8. CONTRACT OR GRANT NUMBER(s)

9. PERFORMING ORGANIZATION NAME AND ADDRESS: U. S. Army Engineer Waterways Experiment Station, Mobility and Environmental Systems Laboratory, P. O. Box 631, Vicksburg, Miss. 39180

10. PROGRAM ELEMENT, PROJECT, TASK AREA & WORK UNIT NUMBERS: Project 4A061101A91D, Task 02, Work Unit 095 06

11. CONTROLLING OFFICE NAME AND ADDRESS: Assistant Secretary of the Army (R&D), Department of the Army, Washington, D. C. 20314

12. REPORT DATE: June 1977

13. NUMBER OF PAGES: 50

14. MONITORING AGENCY NAME & ADDRESS *(if different from Controlling Office)*: Rept. for Sep 75 - Jun 76

15. SECURITY CLASS. *(of this report)*: Unclassified

15a. DECLASSIFICATION/DOWNGRADING SCHEDULE

16. DISTRIBUTION STATEMENT *(of this Report)*: Approved for public release; distribution unlimited.

WES-TR-M-77-2-1

17. DISTRIBUTION STATEMENT *(of the abstract entered in Block 20, if different from Report)*

18. SUPPLEMENTARY NOTES

19. KEY WORDS *(Continue on reverse side if necessary and identify by block number)*
Data acquisition
Landsat (Satellite)
Multispectral data
Remote sensing
Terrain data

20. ABSTRACT *(Continue on reverse side if necessary and identify by block number)*

This report provides an analytical capability for correcting the spectral data, as received by Landsat, to radiance values at ground level. Variations in the radiance values as influenced by atmospheric effects, terrain geometry, and shadows are coupled together to form a single equation that converts the radiance values of images obtained at different times to a common datum.

DD FORM 1 JAN 73 1473 EDITION OF 1 NOV 65 IS OBSOLETE

Unclassified

SECURITY CLASSIFICATION OF THIS PAGE *(When Data Entered)*

038 100

THE CONTENTS OF THIS REPORT ARE NOT TO BE USED FOR ADVERTISING, PUBLICATION, OR PROMOTIONAL PURPOSES. CITATION OF TRADE NAMES DOES NOT CONSTITUTE AN OFFICIAL ENDORSEMENT OR APPROVAL OF THE USE OF SUCH COMMERCIAL PRODUCTS.

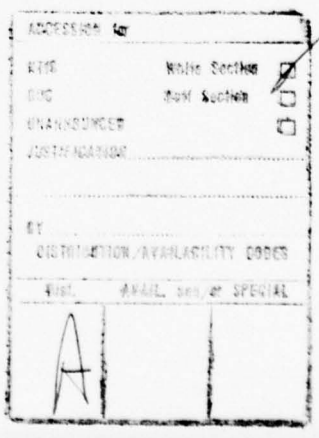

PREFACE

This report is the first of a series dealing with the manipulation and interpretation of Landsat multispectral scanner data. The concepts and procedures reported herein were developed under the In-House Laboratory Independent Research Program, sponsored by the Assistant Secretary of the Army (R&D), Project 4A061101A91D, Task 02, Work Unit 095 Q6, "Feasibility of Using Landsat Spectral Data for Acquisition of Terrain Information for Multiple Purposes." The work was performed during the period September 1975 through June 1976 by personnel of the Environmental Simulation Branch (ESB), Environmental Systems Division (ESD), Mobility and Environmental Systems Laboratory (MESL), U. S. Army Engineer Waterways Experiment Station (WES), under the direct supervision of Messrs. H. W. West, Project Manager, and J. K. Stoll, Chief, ESB. The study was under the general supervision of Messrs. B. O. Benn, Chief, ESD, and W. G. Shockley, Chief, MESL. Dr. H. Struve, ESB, and Mr. W. E. Grabau, Special Assistant, MESL, were responsible for the analytical procedures for making corrections to the Landsat data for the effects of atmospheric attenuation, geometry, and shadows caused by terrain features. Dr. Struve and Messrs. Grabau and West prepared the report.

COL G. H. Hilt, CE, and COL J. L. Cannon, CE, were Directors of the WES during the study and report preparation. Mr. F. R. Brown was Technical Director.

CONTENTS

	Page
PREFACE	2
CONVERSION FACTORS, METRIC (SI) TO U. S. CUSTOMARY AND U. S. CUSTOMARY TO METRIC (SI) UNITS OF MEASUREMENTS	4
PART I: INTRODUCTION	5
Background	5
Objective	7
Ideal Interpretation Procedure	8
PART II: THEORIES AND PROCEDURES FOR HANDLING EXTRINSIC EFFECTS	16
Discussion	16
Atmospheric Effects	17
Effects of Reflectance Geometry	25
Effects of Shadows	32
Consolidated Equation for Extrinsic Effects	39
PART III: POTENTIAL USES	41
PART IV: CONCLUSIONS AND PLANS	44
Comments and Conclusions	44
Plans	45
REFERENCES	46
PLATES 1-4	

CONVERSION FACTORS, METRIC (SI) TO U. S. CUSTOMARY AND
U. S. CUSTOMARY TO METRIC (SI) UNITS OF MEASUREMENT

Units of measurement used in this report can be converted as follows:

Multiply	By	To Obtain
	Metric (SI) to U. S. Customary	
micrometres	3.937007×10^{-5}	inches
centimetres	0.3937007	inches
metres	3.280839	feet
metres	5.399568×10^{-4}	miles (U. S. nautical)
metres	6.213711×10^{-4}	miles (U. S. statute)
kilometres	0.5399568	miles (U. S. nautical)
kilometres	0.6213711	miles (U. S. statute)
square centimetres	0.1550	square inches
square kilometres	0.38610211	square miles (U. S. statute)
	U. S. Customary to Metric (SI)	
degrees (angular)	0.01745329	radians

ACQUISITION OF TERRAIN INFORMATION USING LANDSAT MULTISPECTRAL DATA

CORRECTION OF LANDSAT MULTISPECTRAL DATA FOR EXTRINSIC EFFECTS

PART I: INTRODUCTION

Background

1. There is a dire need for terrain data and related information, particularly geographic intelligence products, for large areas of interest to the military, such as the Middle East, Europe, Southeast Asia, and others. Equally important is the need for terrain information over very large areas for use by the civil sector to detect such things as the extent of flooding, the beginnings of insect infestation in forests or agricultural crops, and illegal encroachments on waterways. For several years, the U. S. Army Engineer Waterways Experiment Station (WES) has been interpreting terrain conditions from aerial photographs; however, this method of terrain data acquisition is quite time-consuming and costly, and other ways of obtaining terrain data are being investigated.

2. There are (1976) two satellites (Landsat 1 and Landsat 2) in orbit around the earth. Each satellite circles the earth approximately every 103 min and contains a multispectral scanner that provides radiance measurements of terrain materials for four spectral bands for discrete areas of the terrain surface. Spectral data for an area on the ground are provided every 18 days by each orbiting satellite, and the two satellites are scheduled such that actual coverage (i.e. spectral data) is obtained every 9 days.* Computer-compatible tapes (CCT's) of

---

* At the time this report was being published, the National Aeronautics and Space Administration (NASA) was in the process of rescheduling the Landsat coverage intervals. After the proposed launch in 1978 of Landsat C, Landsat 1 will follow Landsat 2 six days later, and Landsat C will follow Landsat 2 nine days later.

the spectral data and imagery made from the tapes are made available by the Earth Resources Observation Systems Data Center* approximately 6 weeks after an area has been scanned by the satellite sensor system.

3. The two Landsats, and proposed follow-on satellites, appear to offer an opportunity for acquiring relatively large amounts of terrain intelligence at minimal dollar and time costs, if certain problems of interpretation can be overcome. This report is concerned with one of those problems, namely that of compensating for the effects of the atmosphere, reflectance geometry, and shadows on the character of the spectral data sensed and recorded by the satellites.

4. This is a part of a long-range effort, the objective of which is to develop a capability for interpreting spectral data, as obtained by scanning systems like or similar to those aboard the Landsats, in terms of terrain characteristics and by entirely programmed procedures. It is anticipated that the effort will in fact be truly long-range, chiefly because there is reason to believe that the development of suitable mathematical models for predicting radiance (Block 10, Plate 1, discussed later) will be difficult and time-consuming. In the interim, a "quick-fix" solution to the interpretation problem is badly needed. Such a procedure, based partly on human judgment and partly on computer processing, will be described in detail in Report 2 of this series.[1]

5. As a practical expression of the need for some form of automated (or programmed) interpretation procedure, the Corps of Engineers badly needs a very rapid method of mapping certain relatively crude land-use categories over very large areas (e.g. on the order of 100,000 km^{2}**) at intervals of no greater than 1 year. These maps, representing a time sequence, would be used to determine the actual amounts and locations of land-use categories and the changes in land use between sequences of images, and to establish long-term trends in the

---

* U. S. Department of the Interior, Geological Survey, EROS Data Center, Sioux Falls, S. Dak. 57198.

** A table of factors for converting metric (SI) units of measurement to U. S. customary units and U. S. customary to metric (SI) is presented on page 4.

use of land. Information of this kind is an essential component of the process of flood protection and water resource management planning, as well as of the more immediate need for military terrain intelligence.

6. Although it is easy to state the objective with reasonable succinctness, it is far less easy to rationalize the problem in such a way that the various components or modules can be clearly perceived and defined. In an attempt to do this, a schematic flow diagram has been constructed (Plate 1) that describes, in a very generalized way, the various procedural steps in an ideal programmed interpretation process. The starting point is a Landsat CCT, and the final product is a matrix consisting of pixels (discrete areas on the ground) categorized in some desired fashion. Usually the matrix is written in the form of a map in which the map units are terrain "types" of some kind.

7. It should be carefully noted that the procedure results in categorizations made (i.e., the terrain types have been identified) solely on the basis of spectral analysis. The underlying, but implicit, assumption is that all pixels that exhibit the same spectral distribution of radiance values are representatives of the same terrain type. This assumption is known to be invalid in detail. Nevertheless, in many cases the radiance values exhibited by a specific terrain type tend to cluster so strongly about a common value set that the characteristics of the cluster can be used to identify the terrain type. There is inevitably and in every case a certain amount of misclassification, but it is extraordinarily difficult to determine the precise amount or the precise reasons therefor. A discussion of the problems involved in this area is beyond the purview of this report; some aspects are discussed in Reference 2.

8. This report is the first of a series and deals with selected components of the procedure that is diagrammed in Plate 1.

Objective

9. The objective of this report is to provide an analytical capability for correcting the spectral data, as received by Landsat, to

radiance values at ground level immediately after the radiation has reflected from the terrain surface, and to account for variations in the radiance values as influenced by sun position and topographic configuration (all blocks in Plate 1 except Block 10).

Ideal Interpretation Procedure

CCT radiance values

10. As stated in paragraph 6, the interpretation process begins with the CCT (Block 1, Plate 1). A CCT contains, in multiplexed format, the output of four sensors, each recording in a discrete spectral band, as follows:

Band No.	Wavelength Band, μm
4	0.5-0.6
5	0.6-0.7
6	0.7-0.8
7	0.9-1.1

Each set of four values represents the radiation reaching the satellite from a pixel encompassing an area on the ground approximately 57.2 m wide and 79.1 m long. Two CCT's are required to store all data relevant to each Landsat scene. Each scene represents a parallelogram approximately 185.2 km on a side, or an area of approximately 34,300 km^2. The scene is composed of some 2,340 scan lines, each containing 3,240 pixels,* or a total of 7,581,600 pixels. Since each pixel is represented by one value for each of the four spectral bands, each scene consists of 30,326,400 spectral values.

Correction of CCT radiance values to true radiance values

11. The four values on each CCT that characterize each pixel are not actually true radiance values, but they may be readily corrected to such values (Block 2, Plate 1) by the use of calibration data supplied

---

* These numerical values refer only to Landsat 1. Corresponding values for Landsat 2 vary slightly from those for Landsat 1.

in the header information on each tape. The result is a CCT in which each pixel is defined by four true radiance values, one for each of the four spectral bands (paragraph 10).

Correction of radiance values for atmospheric effects

12. The true radiance values as received at the satellite do not necessarily closely resemble the radiance as it left the ground because the energy has propagated upward through the entire thickness of the atmosphere, with all of its contained gases and particulates. Although the existing methods of accounting for such effects[3] are by no means perfect, they nonetheless are capable of reconstructing the radiance field at ground level with enough reliability to be highly useful (Block 3, Plate 1).

Topographic effects

13. At this point a major problem emerges: in most places, the surface of the earth is far from either flat or horizontal. Except for a relatively few special regions, like parts of the floodplain of the Mississippi River or the beds of playa lakes, the surface of the earth is geometrically complex. The result is that the combination of positions of sun and sensor in the sky produces a relatively complex "reflectance geometry." Even given absolutely uniform surface materials, the north slopes of hills in the mid-latitudes of the northern hemisphere will reflect less light (and thus exhibit a different spectral "signature") than the south-facing slopes. The obvious implication is that the notion that one terrain category is represented by one spectral signature is patently false.

14. This is, in fact, one of the major problems in using the so-called "unsupervised classification" procedures. In these schemes, the radiance sets (i.e., if the data are from Landsat, a "set" consists of the four values defining the spectral composition of a pixel) are grouped into naturalistic clusters. Each cluster is assumed to exhibit a certain coherence; that is, the spectral signatures comprising the cluster do not vary more than a certain amount from each other. This concept clearly has its philosophical origins in the "one material, one signature" assumption.

15. It seems obvious that the assumption must, at a minimum, be altered to read "one material, one condition, one signature." Each change in reflectance geometry clearly produces a different condition and, therefore, a different signature. There are several difficulties in the unsupervised classification procedures, though, even with this assumption. For example, there are as many different signatures as there are variations in slope and aspect angle, since each variation causes at least some change in reflectance geometry. Since the variations in slope and aspect grade into each other in an infinity of variations, at least some terrain configurations could be expected to "smear" the signatures together; the consequence is that a particular landscape type may be represented by a very large, but very loose, cluster of signatures. In practice, this means that there is a high probability of misclassification.

16. Another difficulty inherent in the unsupervised classification procedures arises from the fact that a human must intervene and decide which of the various clusters in fact are expressions of the terrain type of interest. If the assignment is made correctly, it is a simple matter to draw a map in which all of the assigned clusters are labelled as only a single terrain type. The difficulty is that the process involves human photographic interpretation each time an image or data set is processed, and in general this is precisely what needs to be avoided in the interest of time and cost.

Achieving geometric
accordance of CCT images
with topographic base map

17. Before variations in the radiance values as influenced by sun position and topographic configuration can be properly accounted for in the CCT data, geometric accordance must be achieved between the CCT image and a topographic base map. The situation is made significantly complex by two basic factors: the CCT data are recorded in a nonconventional map projection format, and the pixels used by Landsat are not square, whereas most devices for writing images of film are square. Let us consider how these problems may be countered. The route that has

been chosen starts with a base map containing topographic data in the form of contour lines (Block 4, Plate 1). The data represented by the contour lines are converted into a digital data base with the topographic surface represented by a fixed array of points, each labelled with the ground surface elevation at that point (Block 5, Plate 1). The digital data base formatted in this way is referred to as an elevation grid array.

18. At this point, there is a digital topographic map with the grid points arranged according to the particular scale and projection of the original topographic map. The Landsat image, however, as noted above, is not recorded on the same scale or projection. The next step (Block 6, Plate 1) is to bring the image into geometric accordance with the base map, so that there is essentially point-to-point correspondence between them. In principle, geometric accordance could be achieved in a single step by a procedure such as that described in Reference 4. In practice, however, geometric accordance requirements for many applications are less stringent than others and can be achieved somewhat more easily, but less accurately, by the two-stage procedure described below.

19. The spectral data are stored on the CCT's as if the image were to be formed by a strict orthogonal array of pixels. However, since the earth rotates beneath the satellite orbit, the true area covered by a scene is skewed slightly, with the degree of skew related to the latitude of the scene. This error can be largely removed by offsetting each scan line slightly westward. In practice, the skew is corrected by accumulating the small errors between successive scan lines until the error is equal to one pixel width, and then the next scan line (and all subsequent scan lines) is displaced the width of one pixel to the west. In the reformatted tape that results from this process, "false" pixels are added as appropriate to the ends of each scan line, so that the combination of "false" and "real" pixels forms an orthogonal array of pixels. This process adds 260 pixels at the latitude of Vicksburg, Mississippi (specifically $32^{\circ}30'$ N), to each scan line so that the record, reformatted to correct for earth rotational skew, contains 3500 pixels in each scan line. The number of false

pixels needed to orthogonalize the arrays increases as Landsat scenes approach the equator and decreases toward more northern latitudes.

20. Most of the devices used to "write" images on film use perfectly square pixels to form the image. The consequence of this is that an image produced by such a device directly from the skew-corrected record will be significantly shortened in the north-south direction. This is because the Landsat pixel is rectangular and about 21.9 m longer in the north-south direction than in the east-west. If the image is printed with square pixels, it will exhibit a width/length ratio of 0.72 instead of the correct ratio of 1.0. The next step (Block 6, Plate 1) is thus to correct the CCT record for differences in shape between the Landsat pixel and the film-writer pixel. This is normally achieved by adding "false" lines of pixels at appropriate positions. The procedure used simply duplicates each 3d and each 20th scan line. The accumulated error is so small as to be visually indetectable at a map scale of 1:1,000,000.

Construction of map of
slopes and aspect angles

21. Once planimetric accordance is achieved, the image pixel grid is in effect overlaid on the topography, so that the position of each pixel on the landscape has been established. The slope and aspect of the topographic surface under each pixel is then calculated (Block 7, Plate 1) by using a WES computer program[5] called SLOPEMAP. This program accepts as input an elevation grid array representation of the topographic data (paragraph 17), calculates slope and aspect angles for each pixel, and stores their values in an orthogonal array (or map) on a computer magnetic tape.

Correction of radiance
values for reflectance geometry

22. Sidereal time and date at which the image was obtained provide the position of the sun in the sky and, of course, the position of the satellite is also known within narrow limits. These data are then used to correct the received radiance values for the effects imposed by reflectance geometry (i.e. the combined effects of slope and

aspect angles, sun position, and sensor position). In effect, this process "normalizes" the received radiance to the value that would have been exhibited had the topography been perfectly horizontal (Block 8, Plate 1).

23. The procedure currently used, the development of which is described in Part II of this report, assumes that the surface of the earth, regardless of composition, is a perfect Lambertian reflector. This assumption is, of course, invalid. Lack of definitive data on the reflectance characteristics of terrain surfaces has made it impractical to incorporate non-Lambertian reflectance at this time.

Interpretation of radiance values in terms of terrain types

24. The next step is to interpret the normalized radiance value sets in terms of terrain types. At this point the "ideal" procedure, which is the long-range objective, departs even more radically from conventional practice. Conventional practice has two major variants. One is the so-called "unsupervised classification" procedure described in paragraphs 13-16 above. The other basic procedure is the "supervised classification" process. In this, a human operator selects a number of relatively small areas on the ground, which collectively characterize all of the terrain types of interest. These "learning areas" are then submitted to the program, which is designed such that all of the spectral sets in each terrain type, as exhibited within the learning areas, are incorporated as criteria for classification. The spectral data sets for the entire image are then classified according to the criteria derived from the learning areas.

25. One problem is that the learning areas must be selected with great care. For example, all of those specified as representing a given terrain type must include examples exhibiting all topographic variations exhibited by the terrain type. Failure to do so means that the criteria established by the program will be incomplete, and thus the program will misclassify some areas. A second problem is that the learning areas must remain stable over the period of use. If the land use of a learning area is modified between one image and the next, the program will

include the characteristics of the modified area as if they still characterized the original terrain type. The results are sometimes startling. Of course, the learning areas can be updated, but only at the expense of human intervention.

26. It should be noted that both of the conventional methods require considerable human intervention, including some subjective image interpretation, each time the procedure is used. The ideal procedure must avoid this requirement, if at all possible. The problem is to develop a procedure that will make it possible to specify recognition criteria for terrain types such that the criteria are independent of the individual image characteristics. In effect, we must be able to specify to the interpretation program that a given terrain feature will be characterized by a particular set of spectral values under the conditions obtained during image acquisition. Further, those criteria must have been derived by a process independent of the image acquisition process.

27. The ideal procedure that has been hypothesized begins (Block 9, Plate 1) with the reflectance characteristics of terrain features. The critical point is that, for most terrain features, there is no such thing as a "spectral signature" in the sense that there is (for example) a particular set of radiance values that is characteristic of an oak forest. Instead, the reflectance characteristics of the individual leaves (and therefore of the forest as a whole) change at least as a function of seasonal growth stage, state of soil moisture, and health. The reflectance characteristics of the upper surface of the canopy change as a function of sun angle, because such changes alter the proportion of the surface in shadow.

28. Despite all of these complexities, there is a thread of unity; the changes are regular and, to a large degree, predictable. The essential technical problem is therefore to develop what might be called "reflectance prediction models" of the terrain types of interest. Such models would require weather history, state of the atmosphere at the appropriate time, and lighting conditions as input and would yield a prediction of spectral radiance at the time of satellite overpass (Block 10, Plate 1).

29. Given the normalized radiance data available at the end of the image processing schedule previously described, the interpretation program would then search the image spectral sets and match each pixel set against the predicted values (Block 11, Plate 1). A match would be tantamount to classification, and thus the result would then be output as a map of the distribution of the desired terrain types (Block 12, Plate 1).

PART II: THEORIES AND PROCEDURES FOR HANDLING EXTRINSIC EFFECTS

Discussion

30. Paragraph 12 mentioned that the spectral data recorded by the Landsat sensor system only indirectly represents the spectral characteristics of the energy at the surface immediately after reflectance. This is because the radiation has had to propagate upward through the entire thickness of the earth's atmosphere, with all of its constituent gases and suspended particulates. Both the gases and particulates extract a toll, through absorption and scattering, and thus the energy emerging at the top of the atmosphere is always materially less than at the bottom.

31. Even if there were no atmosphere, the received radiation would nearly always exhibit less energy than the reflectance of the materials at the earth's surface would suggest. This is because the surface materials are nearly always inclined at some angle with respect to both source and sensor, and thus the satellite "sees" a surface inclined at some angle other than the optimum reflectance angle. That is, variations in reflectance geometry modify the apparent reflectivity of terrain surfaces.

32. Finally, the topography can act almost in the capacity of an on-off switch. If the terrain exhibits slope angles greater than the solar elevation angle, and if the aspect of the slopes is away from the sun, then some of the slopes, as well as some of the adjacent terrain, will be in shadow. To be sure, this area is illuminated by scattered light from the sky, but the level of illumination is usually so low that virtually all detail is lost. Furthermore, the light from the sky does not have the same spectral composition as light directly from the sun. The result is that the light reflected from the terrain surfaces of regions in topographic (or cloud) shadows exhibits quite different spectral compositions than does the light reflected from similar terrain conditions directly illuminated by the sun.

33. The effects of the three extrinsic effects described above (i.e. atmospheric effects, effects of topography and sun position, and

effects of terrain shadows) are so large that they must be accounted for before the Landsat radiance data can be interpreted in terms of type and characteristics of terrain materials. The development of procedures to achieve this goal is described below.

Atmospheric Effects

Theory

34. Atmospheric effects on incident and reflected radiation are illustrated in highly schematic form in Figure 1. From the instant solar radiation arrives at the top of the earth's atmosphere (Figure 2), its radiation flux density (or radiation intensity) is reduced. Two principal mechanisms are involved: molecular absorption and scattering, and aerosol (or particulate) absorption and scattering. The first depends on the gaseous composition (primarily oxygen, nitrogen, water vapor, ozone, and carbon dioxide) and density. Since both composition and density vary with altitude (measured from mean sea level as a datum), seasons of the year, and latitude, different layers of the atmosphere exhibit somewhat different molecular absorption and scattering properties.

35. The second mechanism, aerosol absorption and scattering, depends on the types and concentrations of particulates suspended in the atmosphere. As with gases, these are nonuniformly distributed through the depth of the atmosphere and vary with season and latitude as well.

36. Thus, different atmospheric layers result in different amounts of absorption and scattering. The consequence is that the atmospheric transmittance of solar radiation is significantly different in summer and winter at all latitudes, and it differs as a function of latitude independent of season.

37. Still another complexity arises from the fact that local weather conditions may change the local concentration of suspended particulates. Nearly everyone has had experience with dust storms, smog, and fog. In extreme cases, the effects of such localized conditions may be larger than all other effects combined. Thus, it is of

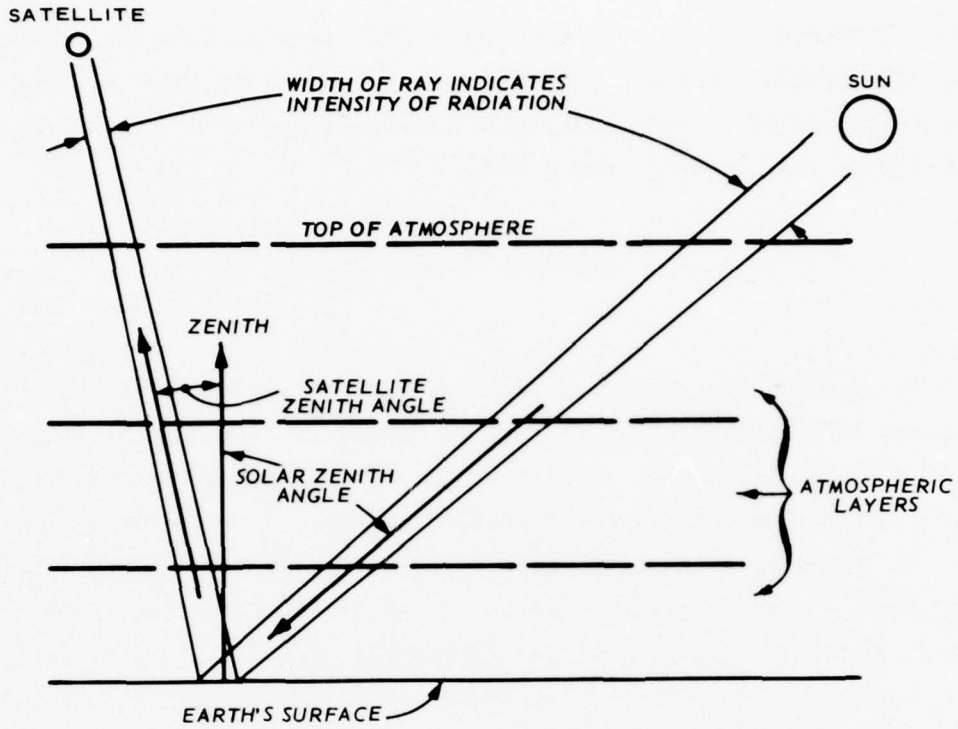

Figure 1. Schematic diagram of radiation intensity losses along incident and reflected atmospheric paths

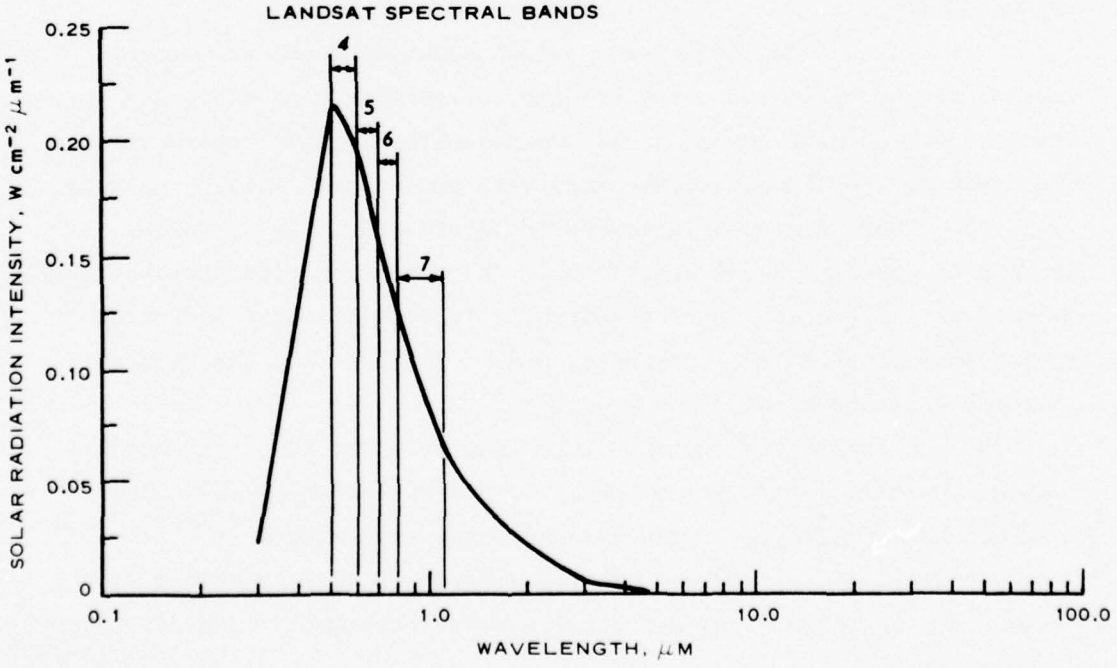

Figure 2. Solar spectral distribution above earth's atmosphere

critical importance that some definition of local atmospheric conditions be specified.

38. One of the best available procedures for obtaining quantitative estimates of the radiation losses caused by the complex of atmosphere-controlled processes described above is a mathematical atmospheric transmittance model (LOWTRAN 2) developed at the U. S. Air Force Cambridge Research Laboratory. The model is described in detail in Reference 6. In brief, LOWTRAN 2 derives a transmittance coefficient for each atmospheric layer for each season, latitude, and local atmospheric condition (called a "haze" condition). Refraction and earth curvature effects are also included. Since the effects on each wavelength are somewhat different, a transmittance coefficient is calculated for each wavelength.

39. The transmittance coefficient is essentially a ratio between radiation flux densities: the radiation intensity at a given wavelength (λ) is measured as the radiation enters a specific column of atmosphere (I_1) and again as it leaves the column (I_2), and the transmittance coefficient is then the ratio I_2/I_1. LOWTRAN 2 produces a transmittance coefficient for each wavelength for each atmospheric layer for three latitude regions (tropic, mid-latitude, and arctic), two seasons (summer and winter), and two haze conditions (5-km horizontal visibility and 23-km horizontal visibility). The basic product of the model is a specification of the effective sum of the transmittance coefficients through the entire atmosphere as a function of wavelength (Figure 3), with a wavelength resolution of 20 wave numbers (wave number is defined as $k = 1/\lambda$, where λ is expressed in centimetres).

40. The spectral resolution provided by LOWTRAN 2 is much greater than is required for analysis of Landsat data. The Landsat sensor uses four relatively broad spectral bands, as described in paragraph 10. Thus, for use in Landsat applications, the very narrow spectral bands used in LOWTRAN 2 must be integrated into the four broad Landsat bands. The four Landsat spectral bands are indicated in Figure 3. Note that the percent transmission (= transmittance coefficient) values characteristic of the Landsat spectral bands differ significantly. For example,

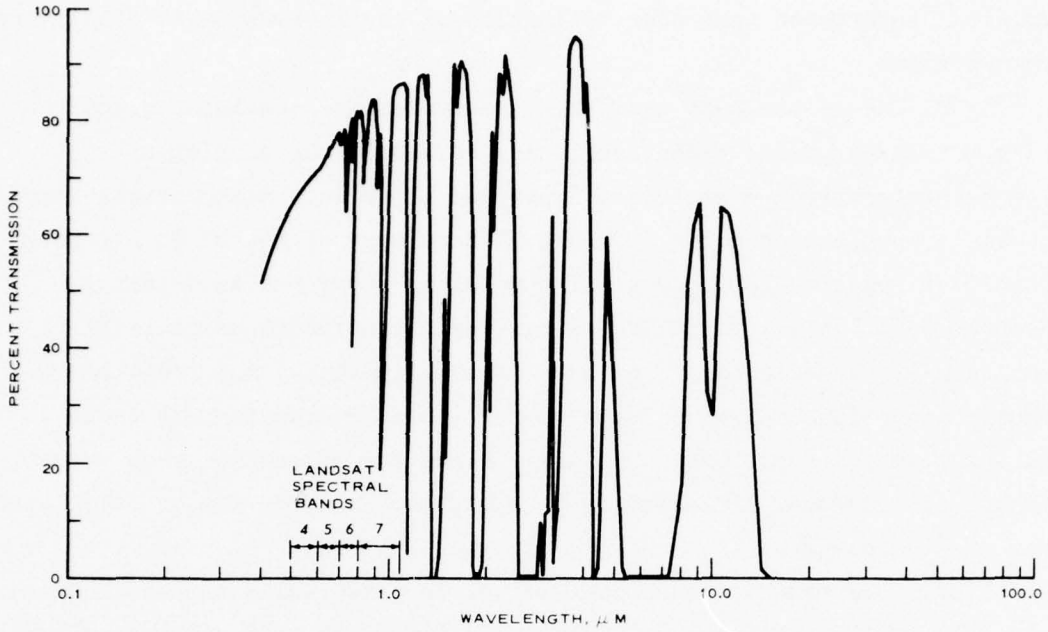

Figure 3. Atmospheric transmission probability for a clear mid-latitude summer geographic atmosphere. The probabilities were calculated for radiation transmitted through the entire atmosphere along a vertical path

the approximate average for band 4 is 70 percent, and that for band 5 is about 75 percent.

41. These integrated values change rather substantially with changes in the solar zenith angle (i.e. seasons). For example, Figures 4 and 5 illustrate the changes in values as a function of solar zenith angle for mid-latitude winter and summer, respectively. The curves were calculated for a haze-free condition for all four spectral bands of Landsat.

42. In general, winter atmospheres are more transparent than summer atmospheres in mid-latitudes, and thus winter atmospheric transmission values are greater than summer values. Note that the values for each Landsat spectral band (labelled accordingly in Figures 4 and 5) are quite different for summer and winter atmospheres.

43. As an illustration of the relative changes in atmospheric transmission from one season of the year to the next, a "normalization factor" can be derived from the coefficients. The graph in Figure 6

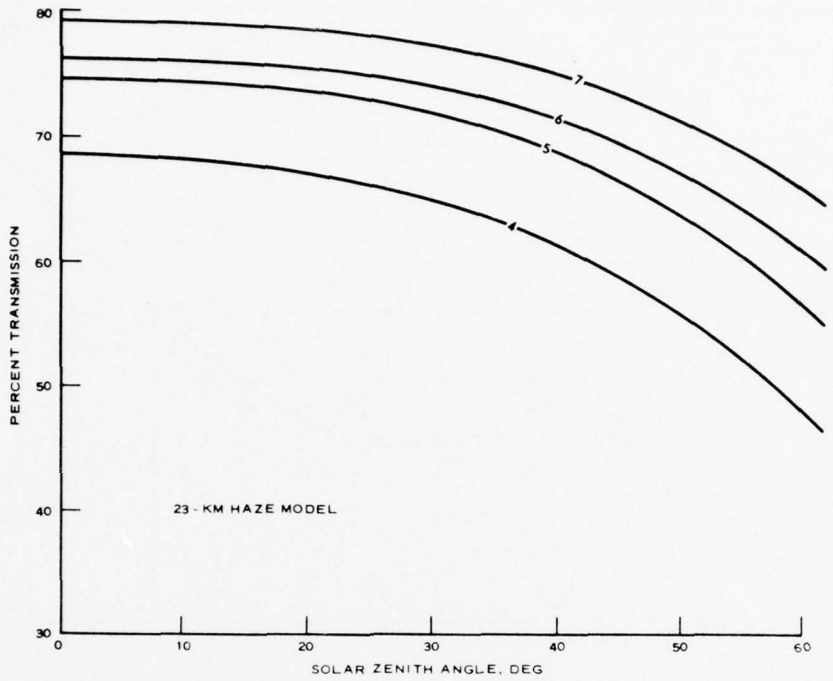

Figure 4. Mid-latitude winter atmospheric transmission values for Landsat spectral bands 4, 5, 6, and 7

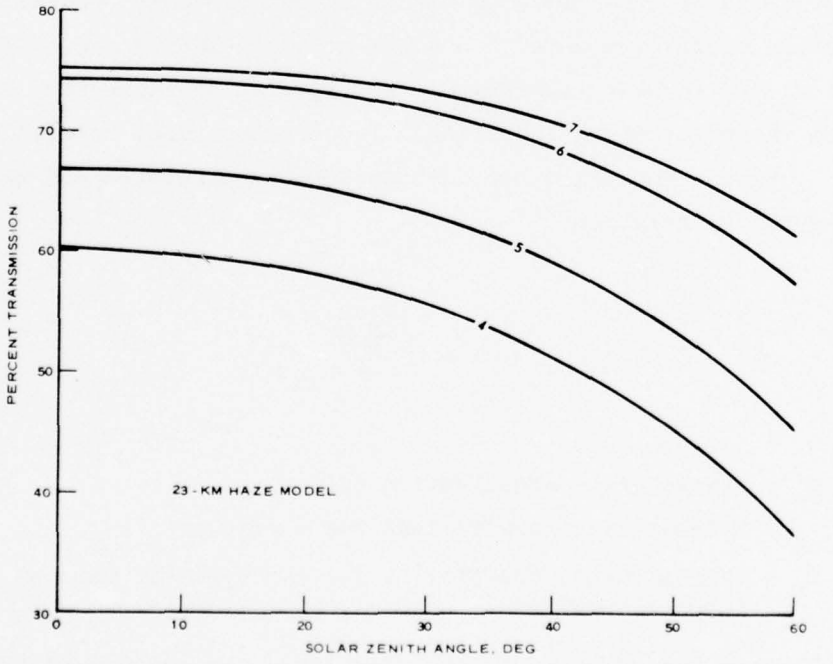

Figure 5. Mid-latitude summer atmospheric transmission values for Landsat spectral bands 4, 5, 6, and 7

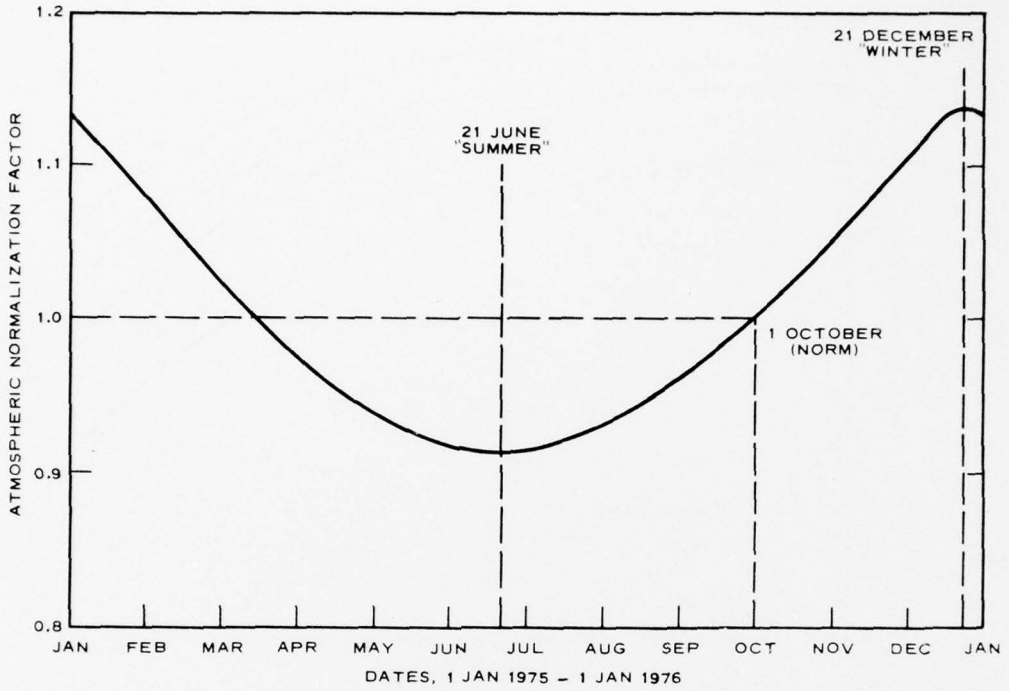

Figure 6. Atmospheric normalization factor for Landsat band 6

was constructed by the following normalization process. The atmospheric transmission coefficients for 1 October at a mid-latitude location were calculated by using LOWTRAN 2, and those values were then assumed to be the "norm" or index condition. The transmittance coefficients for that latitude for all other days were then calculated and normalized according to the relation

$$F_A = \frac{T_{oct}}{T_t} \tag{1}$$

where

F_A = atmospheric normalization factor

T_{oct} = transmittance coefficient for 1 October

T_t = transmittance coefficient for any specific date as calculated by LOWTRAN 2

Since 1 October was selected as the norm date, the product of the October

atmospheric normalization factor for any date and the radiance values obtained on that date have the effect of removing variations in the radiance values attributable to differences in the atmospheres of the two dates (specifically, the given date and 1 October). For example, to remove the variations in the Landsat band-6 radiance values due to 1 January and 1 October atmospheric differences, the band-6 radiance values obtained on 1 January should be multiplied by a normalization factor of 1.13 (Figure 6). This factor represents a relative variation of 13 percent in these radiance values and emphasizes the fact that atmospheric effects are often significant, and methods for compensating for them must be included in the ideal image interpretation system (Plate 1).

Procedure

44. The theoretical considerations described above can be readily converted into a procedure for achieving the process specified in Block 3 of Plate 1, namely that of correcting the radiance values as received at the satellite for atmospheric effects. The procedure given diagrammatically in Plate 2, is as follows:

a. First, determine the latitude of the Landsat scene (usually the center of the scene is chosen), and the date and time at which it was obtained (Block 3.1, Plate 2). These data are all available from header information on the CCT's supplied by the EROS Data Center, Sioux Falls, S. Dak.

b. Locate the nearest weather station at which ground visibility conditions are recorded, and obtain the horizontal visibility data obtained at the time closest to that at which the Landsat image was obtained. Since weather stations frequently record visibility in terms of miles, one must first convert this parameter to kilometres before it is acceptable to LOWTRAN 2 (Block 3.2, Plate 2).

c. Determine the mean elevation of the geographic region covered by the Landsat scene (Block 3.3, Plate 2).

d. Using LOWTRAN 2, calculate the atmospheric transmission coefficients along the path of reflected radiation for each of the four Landsat wavelength bands, using the haze condition obtained in step b above, the latitude and date information obtained in step a above, and the mean elevation of the scene in step c above (Block 3.4, Plate 2).

e. Since Landsat is looking virtually straight down at the earth's surface, the satellite zenith angle is assumed equal to 0 deg. Multiply the radiance values defining each pixel (Block 3, Plate 1) by the reciprocal of the appropriate atmospheric transmittance coefficients, as calculated in step d above (Block 3.5, Plate 2).

f. The product is a new CCT, formatted in precisely the same way as before, but containing the radiance values on a pixel-by-pixel basis of all four spectral bands, as if those values had been obtained as the radiation left the ground and started upward through the atmosphere on its way to the satellite sensor (Block 3.6, Plate 2).

45. Note that Plate 2 illustrates two procedures that diverge immediately after Block 3.4 (in which the atmospheric transmittance coefficients are calculated). The first procedure (Blocks 3.4-3.6), described in the preceding paragraph, back-calculates from the radiance values perceived by the satellite sensor to the values at ground level immediately after the rays have reflected from the terrain surface. The second procedure (Blocks 3.7-3.10) determines the intensity of solar radiation at ground level just before the energy reflects from the terrain surface. Note that in Plate 1, Block 10, a prediction of radiance values for terrain categories will require a specification of the intensity of the radiation illuminating those categories. Thus, the second procedure described in Plate 2 is an essential component of the "ideal" image interpretation system. In detail, the procedure (starting after Block 3.6, Plate 2), is as follows:

a. Obtain, from any standard ephemeris, the solar zenith angle for the appropriate place (Block 3.7, Plate 2). If the entire Landsat scene is to be processed, the center of the scene is normally chosen.

b. Using LOWTRAN 2, calculate the atmospheric transmission coefficients along the path of incident radiation for each of the four Landsat spectral bands, using the data obtained on steps a, b, and c in paragraph 44 above (Block 3.8, Plate 2).

c. Multiply the solar constant radiance values by the transmittance coefficients (Block 3.9, Plate 2).

d. The product is a wavelength-by-wavelength definition of the solar radiance at ground level (Block 3.10, Plate 2). Note that it does not include consideration of the so-called sky radiation; that is, the down-welling light

scattered from atmospheric constituents. This light source is not considered in the procedure under discussion.

46. It should be noted that the two procedures use two different "transmittance coefficients." The first procedure, described in paragraph 44, uses a transmittance coefficient describing the fraction of radiation transmitted along a vertical path through the atmosphere, which is a reasonable approximation of the path from earth to satellite. This coefficient is designated $T_r(\lambda,\phi_{sat})$, where λ is the wavelength and ϕ_{sat} is the satellite zenith angle. In all cases described thus far, ϕ_{sat} equals 0 deg.

47. The second procedure, described in paragraph 45, uses a transmittance coefficient describing the fraction of radiation transmitted along a slant path through the atmosphere and is designated $T_i(\lambda,\phi_{sun})$, where ϕ_{sun} is the solar zenith angle.

Effects of Reflectance Geometry

Theory

48. Again, in the "ideal" image interpretation system (Block 10, Plate 1), it will be noted that a prediction of radiance values for terrain categories will require a specification of the exact conditions at the time of image acquisition. That is, the slope and aspect angles, as well as sun and sensor positions, must be known accurately. However, since these geometric quantities have such a complicated effect on the radiance reaching the satellite sensor, it is extremely difficult, in general, to develop an explicit mathematical expression that describes the reflectance relation between the incident and reflected radiant flux. The relation, or so-called "in situ signature," can, however, be expressed implicitly (assuming no terrain polarization effects) by

$$\rho(\lambda,\alpha,\beta) = \frac{I_r(\lambda,\beta)}{I_i(\lambda,\alpha)} \qquad (2)$$

where

$\rho(\lambda,\alpha,\beta)$ = the reflectance signature for the in situ terrain material at the surface with respect to the given wavelength λ, and conditions α and β at the time of the image acquisition

$I_r(\lambda,\beta)$ = reflected terrain radiance values at the surface for the given wavelength λ and angle of reflectance β

$I_i(\lambda,\alpha)$ = incident solar radiance values at the surface for the given wavelength λ and angle of incidence α

The geometric relation for this quantity is shown in Figure 7.

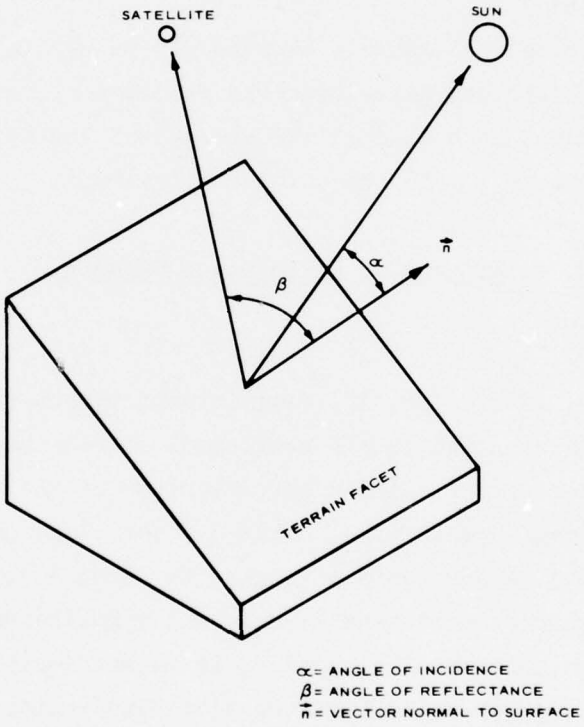

Figure 7. Definitions of angles involved in reflectance geometry

49. If the surface on which the incident radiation strikes is assumed to be a perfectly diffuse reflector (i.e. a perfect Lambertian surface), then the implicit reflectance relation for the in situ signature $\rho(\lambda,\alpha,\beta)$ is greatly simplified and is given by

$$\rho(\lambda) \cong \frac{I_r(\lambda)}{I_i(\lambda)\ S(\alpha)} \tag{3}$$

where

$S(\alpha)$ = slope attenuation coefficient, which takes into account the slope and aspect angles and sun position

50. The effects on perceived radiance caused by variations in reflectance geometry are very large. The magnitude may be qualitatively anticipated by noting that a south-facing slope at a mid-latitude (such as $32^{\circ}30'$ N at Vicksburg, Mississippi) will be exposed to beams almost parallel to the surface, but opposite in direction at dawn and sunset, and yet illuminated by almost perpendicular rays at noon. A sensor looking vertically down at such a slope will obviously receive quite different amounts of radiation during the course of a day. Nor will the daily cycle exactly repeat because the solar zenith angle changes with the progression of the seasons. That is, the angle of incidence (α in Equation 3) on a given slope facet changes as a function of date and time.

51. The assumption that natural terrain surfaces are true Lambertian reflectors is obviously invalid. Instead, it seems likely that all, or nearly all, have preferred reflectance directions. However, in the absence of definitive data on the types and amounts, non-Lambertian effects cannot be incorporated at this time.

52. The slope attenuation coefficient in paragraph 49 above can be mathematically expressed in terms of the cosine of the angle of incidence α and is written

$$S(\alpha) = \cos \alpha \tag{4}$$

where

$\cos \alpha = \sin \phi_{sun} \sin \phi_n \cos(\theta_{sun} - \theta_n) + \cos \phi_{sun} \cos \phi_n$

ϕ_{sun} = solar zenith angle or the angle between the solar position vector (i.e. a vector directed toward the sun) and zenith

ϕ_n = terrain slope angle or angle between a vector normal to the terrain (slope vector) and zenith

θ_{sun} = solar azimuth angle or the horizontal clockwise angle

between true north and the projection of the solar position vector on the horizontal plane

θ_n = terrain aspect angle or horizontal clockwise angle between true north and the projection of the slope vector on the horizontal plane

The geometrics of the slope and solar vectors described above are illustrated in Figure 8. The explicit expression above for cos α was derived using the definition of the dot product of the two vectors $\vec{s}$ and $\vec{n}$ shown in Figure 8.

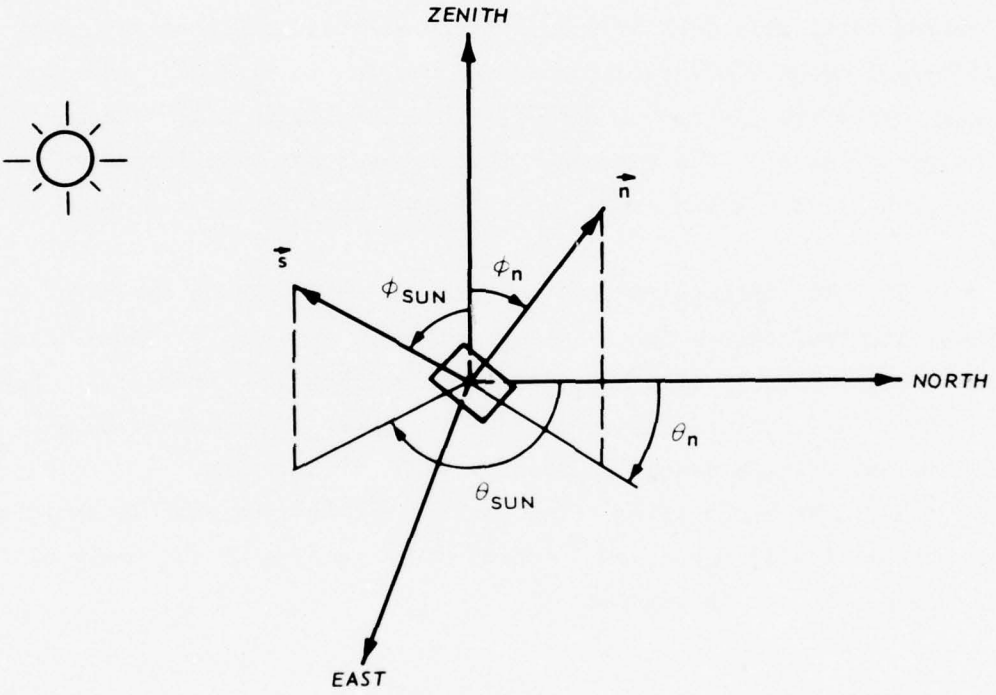

Figure 8. Illustration of the zenith (ϕ_{sun}) and azimuth (θ_{sun}) angles defining the solar position vector $\vec{s}$ and the slope (ϕ_n) and aspect (θ_n) angles defining the slope vector $\vec{n}$

Procedure

53. The procedure described below (Plate 3) is an expansion of Block 8, Plate 1, and is thus a part of the "ideal" interpretation system:

a. First, determine the slope and aspect angles (Block 8.1, Plate 3). This will be obtained as a derivation from a

topographic base map in the "ideal" system (Block 7, Plate 1). A detailed procedure for determining slope data from topographic maps has been developed by the WES as discussed in Reference 5.

b. From any standard ephemeris, determine the solar zenith and azimuth angles for the time at which the Landsat image was obtained (Block 8.2, Plate 3).

c. Solve Equation 4 to obtain the slope attenuation coefficient (Block 8.3, Plate 3). This calculation is made for each pixel in the scene, since each is presumed to have unique slope and aspect angles.

d. Multiply each of the set of four values defining the received radiance of each pixel by the attenuation coefficient derived for that pixel (Block 8.4, Plate 3).

e. The product is a new set of radiance values for each pixel. The calculated values are those that would have been exhibited had the reflecting surface been perfectly horizontal with the sun at zenith (Block 8.5, Plate 3). In effect, all radiance values have been normalized to a common datum.

54. Figure 9 illustrates the dependence of the attenuation coefficient on slope angle, slope aspect, and solar zenith and azimuth angles. The three curves labelled JUL, OCT, and FEB represent the effects of solar zenith and azimuth at a location near Vicksburg, Mississippi, at the time of Landsat overpasses on 11 July 1974, 13 October 1974, and 21 February 1975, respectively. The corresponding sun azimuth angles (rounded to the nearest degree) are 31, 49, and 55 deg, respectively.

55. The attenuation coefficient may also be used to derive a "normalization factor." As an example, assume a slope of 10 deg with an aspect angle of 280 deg. Then, for the same time of day, the attenuation coefficient for the selected slope facet will march regularly with the seasons. If the attenuation coefficient of a particular day is selected, as a norm, as for example 1 October, then the ratio of attenuation coefficients for all other days to that of 1 October may be considered to be a normalization factor:

$$F_s = \frac{S_{oct}}{S_t} \tag{5}$$

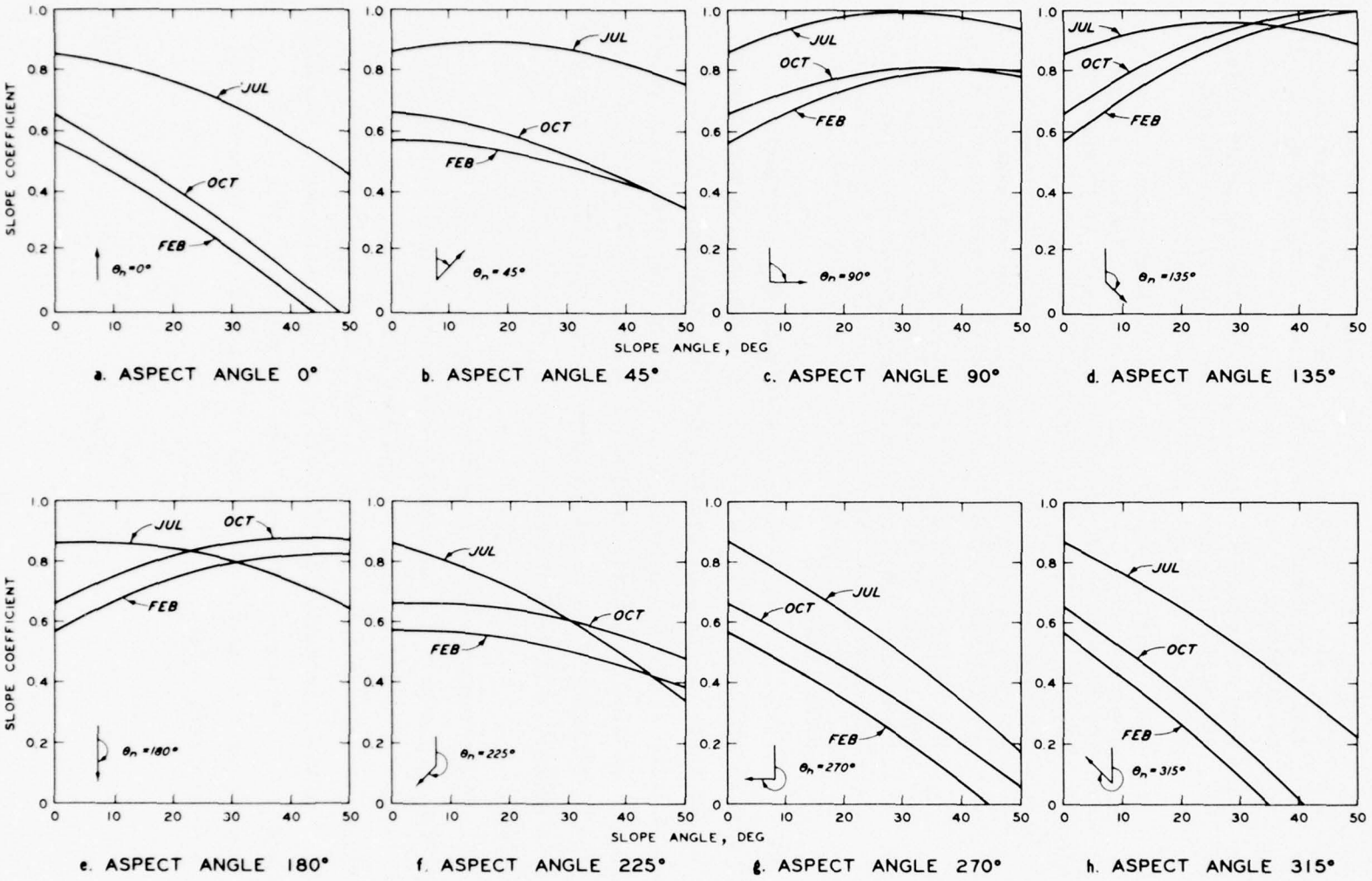

Figure 9. Slope attenuation coefficients for 11 July 1974, 13 October 1974, and 21 February 1975, calculated for eight aspect angles and an angle of reflectance of 0 deg ($\beta = 0$)

where

F_s = slope normalization factor

S_{oct} = the attenuation coefficient for 1 October at 0942 hr (nominal local time of Landsat overpasses at Vicksburg, Mississippi)

S_t = the attenuation coefficient for any day of the year at 0942 hr

A result of this process, using the values in the previous example, is shown in Figure 10. Since the slope is facing slightly north of west (aspect 280 deg), the sun at 0942 hr will be almost "behind" the slope facet, as well as low in the sky. The result is that the attenuation coefficient will be very high. By July, the sun will be much higher in the sky at 0942 hr, and thus the attenuation coefficient will be low. If 1 October is selected as the norm, as in Figure 10, the product of the normalization factor for any date and the radiance values obtained on that date will bring those radiance values to the value that would be

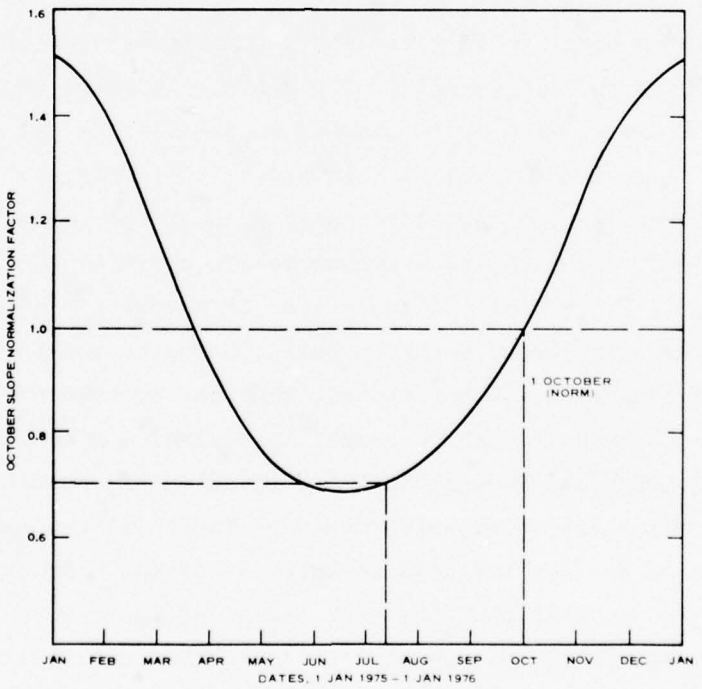

Figure 10. October slope normalization factors for 1975. Curve was calculated for slope and aspect angles of 10 and 280 deg, respectively

exhibited on 1 October. For example, radiance values measured on a facet with a slope of 10 deg and an aspect of 280 deg on 15 July at 0942 hours, then multiplied by a normalization factor of about 0.7, would result in new radiance values that would be those expected on the same facet on an image obtained on 1 October, assuming, of course, that conditions on the ground had not changed in the meantime.

Effects of Shadows

Theory

56. As previously discussed in paragraph 32, the radiance levels in shadows, recorded as parts of a Landsat image, are so low that it is very difficult, and in many instances impossible, to obtain a useful set of spectral values from them. The result is that the radiance value sets coming from "shadow" pixels cannot be used for classifying terrain types. The most useful thing that can be done at this time is to remove them from the record, so they are not a possible source of confusion.

57. Only shadows caused by topographic features are considered in this study. Clouds also cause shadows on the terrain, of course, but they are not considered; all Landsat scenes currently used at the WES are cloud-free. Vegetation also causes troublesome shadows under certain circumstances. For example, a forest margin oriented at right angles to the azimuth of the sun will cause a line of shadow if the sun is over the forest. If the trees are 20 m tall, the solar zenith angle is 70 deg, and the ground is horizontal, the zone of shadow will be about 55 m wide, just wide enough to result in a pixel dominated by shadow effects, if the pixel happens to be centered on the shadow zone. However, such cases are relatively rare, and for this reason vegetation-caused shadows are not included in this discussion. Nevertheless, it should be kept in mind that the effect will almost always produce at least a few pixels on any one Landsat scene that will yield anomalous interpretations. That is, they will produce errors in identification and classification.

58. Four basic conditions or situations can produce shadows. The

first of these depends on the relative position of the sun with respect to a slope facet. If the slope facet faces away from the sun, and the slope is greater than the solar zenith angle, then the facet will be in shadow. This condition occurs when the value of $\cos \alpha$ in Equation 4 is a negative number.

59. The second basic condition depends on the interposition of a topographic feature into the line of sight connecting the point of interest on the ground and the sun. In other words, the question is: Is there a hill that casts a shadow on the ground? This condition can be mathematically determined by writing an equation describing the line of sight between the pixel of interest and the sun, and then determining whether any point along that line exhibits an elevation greater than the line. If so, it obstructs the line of sight and the pixel of interest will be in shadow.

60. The third condition is not really a shadow effect at all, at least in the conventional sense. It depends on the position of the satellite with respect to the topographic surface. In effect, the question is: Can the satellite see the topographic surface? This condition occurs when the cosine of the reflectance angle β is negative. The value of $\cos \beta$ can be calculated from the expression

$$\cos \beta = \sin \phi_{sat} \sin \phi_n \cos(\theta_{sat} - \theta_n) + \cos \phi_{sat} \cos \phi_n \qquad (6)$$

where

ϕ_{sat} = satellite zenith angle, or the angle between the satellite position vector (i.e. a vector directed toward the satellite) and zenith

θ_{sat} = satellite azimuth angle, or the horizontal clockwise angle between true north and the projection of the satellite position vector on the horizontal plane

The angles ϕ_n and θ_n are, respectively, the terrain slope and aspect angles and are defined as before (paragraph 52).

61. The fourth basic condition is analogous to the second, except that the line of sight is that connecting the ground surface with the satellite, rather than with the sun.

62. The third and fourth conditions described above are not significant when using Landsat imagery. The reason is that the satellite is at the zenith, and thus few topographic surfaces are hidden from view. Nevertheless, the possibility of concealment exists. It will be recalled that the Landsat satellite is not at the zenith when receiving radiation from pixels other than those along the orbital track. When receiving radiation from pixels at the end of the scan line, the satellite is actually about 5.6 deg away from the zenith. Thus, the face of a cliff with a slope exceeding about 84.4 deg would be out of view of the Landsat satellite if it was facing away from the satellite ground track and located at the edge of the scanned zone. The face of Halfdome in Yosemite National Park might meet this criterion, for example.

63. Clearly, the shadow conditions based on satellite position are not included because of Landsat. Instead, they are included because it is anticipated that the procedures will be used eventually for the analysis of data from airborne scanners, including sidescan radars. Some of these sensor systems have very wide scan angles, so that the angle of incidence of the lines of sight at the edges of the scanned zone are quite small. In such cases, the "shadow zones" may be quite extensive. In this case, two sets of imagery of the same area, but taken from two different flight tracks, will not necessarily exhibit paired data from all locations. Analytical procedures based on such pairs will thus be inapplicable for regions in view only from one flight track.

Procedure

64. The generalized schematic of the procedure, given in Plate 4, is an expansion of Block 8, Plate 1. Note that the points of beginning (i.e. determination of slope and aspect angles (Block 8.1) and solar zenith and azimuth angles (Block 8.2)) are exactly the same as the points of departure for the reflectance geometry procedure (Plate 3).

a. Calculate (Block 8.3, Plate 4) the cosine of the angle α (angle of incidence of solar ray on the surface of interest; see paragraph 52). If the value of $\cos \alpha$ is greater than 0 (i.e., is a positive number), the pixel under examination is coded with a 1 , to indicate

that it is illuminated by the sun, unless it is shadowed by another part of the topography. If the value of $\cos \alpha$ is zero or a negative number, the pixel is in shadow, and it is therefore coded with a 0, which removes it from further consideration.

b. If the pixel is coded 1, write an equation defining a line of sight from the center of the pixel under examination to the center of the sun (Block 8.6, Plate 4). The equation can be visualized as representing a line lying in a vertical plane passing through the earth. The topographic surface can then be visualized as a trace in that same plane. The procedure (Block 8.7, Plate 4) is to compare elevations along the trace of the topographic surface (E_t) with the elevations of the line of sight (E_{los}) at the same horizontal distances from the pixel. If at any point $E_t \geq E_{los}$, the pixel will be in shadow, and the pixel is coded 0, which removes it from further consideration. If $E_t < E_{los}$ for all points along the line, the pixel is coded 1, and is assumed to be illuminated.

c. Determine the sensor zenith and azimuth angles (Block 8.8, Plate 4), and, with the slope and aspect angles (Block 8.1, Plate 4), determine (Block 8.9, Plate 4) the cosine of the angle β (angle of reflectance, see paragraph 60). If $\cos \beta$ is a positive number ($\cos \beta > 0$), the pixel under examination is coded 1, which means that it can be seen from the sensor, unless it is obscured by another topographic feature. If $\cos \beta$ is zero or a negative number ($\cos \beta \leq 0$), the pixel is not within line of sight of the sensor and is coded 0, which removes it from further consideration.

d. Write the equation for the line of sight connecting the center of the pixel and the sensor (Block 8.10, Plate 4). In a process analogous to that described in item b above, the presence or absence of obstructing topography along the line of sight is determined (Block 8.11, Plate 4). If $E_t \geq E_{los}$ at any point along the line of sight, the pixel cannot be seen from the sensor and is coded 0 and removed from consideration. If $E_t < E_{los}$ for all points along the line, the pixel is visible from the sensor and coded 1 to indicate that it remains a part of the data field subject to further analysis.

65. To demonstrate the algorithm that was developed for the shadow calculations, a 2- by 2-km site was selected. Computer line plots of the site are shown in Figure 11. Lines of sight were calculated for the site using an elevation data array (Block 5, Plate 1) that

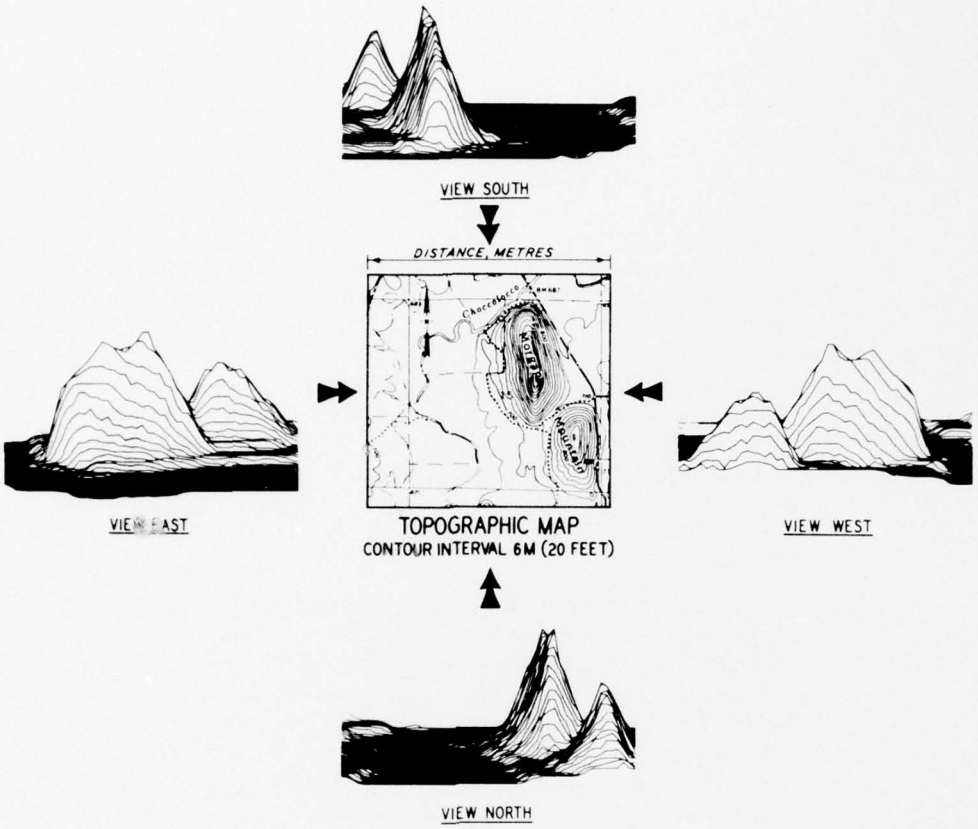

Figure 11. Perspective views and topographic map of the shadow algorithm study site

had a grid spacing of 39.5 m (one-half the length of a Landsat pixel). Results of these calculations are shown graphically in Figures 12 and 13. Figure 12 shows the results for a sun elevation angle of 15 deg and two different sun azimuths (90 and 45 deg); whereas, Figure 13 shows the results for three different sun elevation angles (15, 30, and 45 deg) at a common sun azimuth (90 deg). Note that the number of pixels in shadow is different for the different sun elevation and azimuth angles. For the calculation (Figure 12) with a sun elevation of 15 deg and a 90-deg sun azimuth, 642 Landsat pixels representing 1.00 km^2 of area were determined to be in shadow; whereas for the 45-deg sun azimuth, 548 pixels representing 0.86 km^2 of area were determined to be in shadow. In the case of different sun elevation angles and a 90-deg sun azimuth

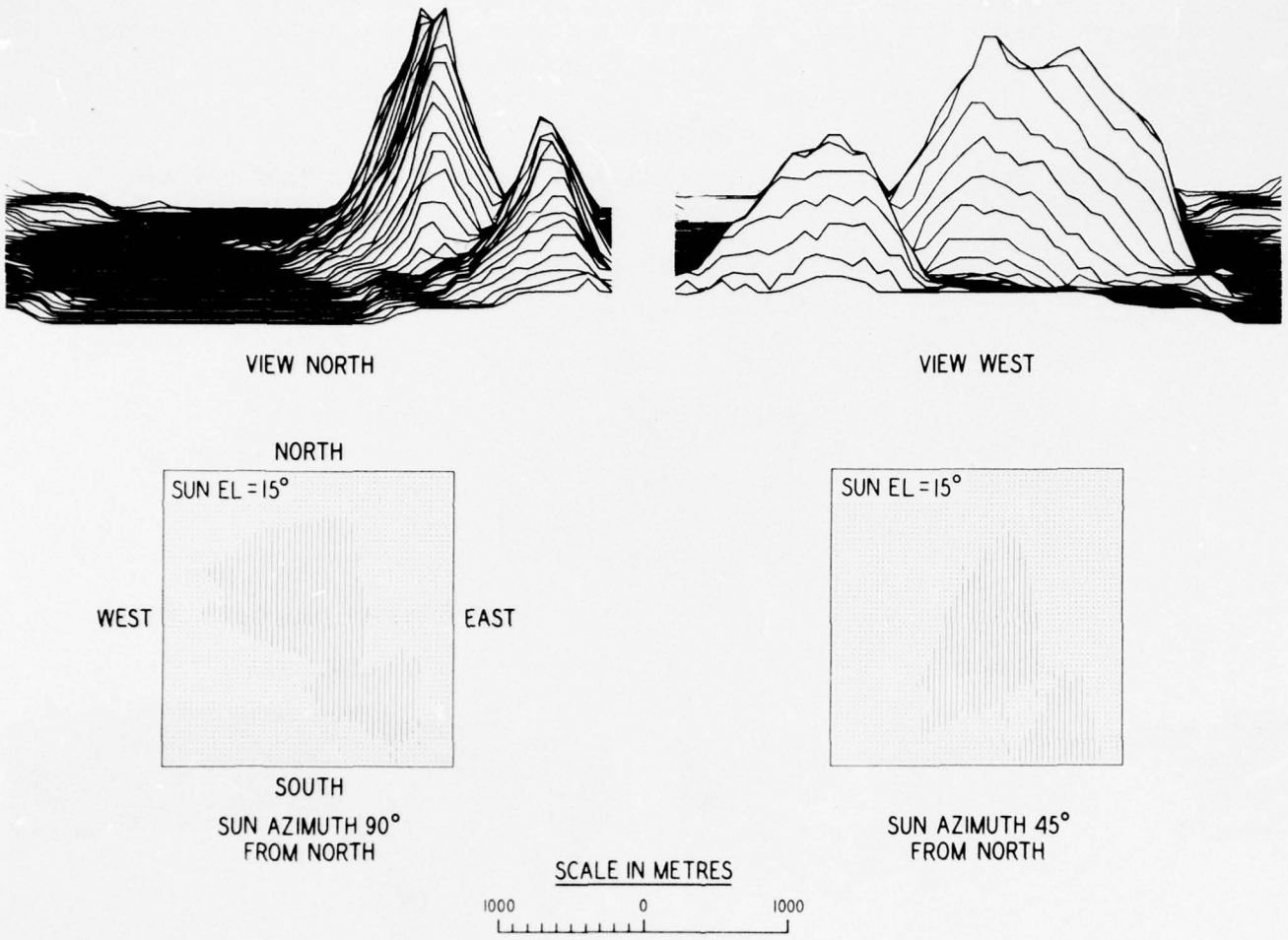

Figure 12. Ground area in shadow for a common sun elevation angle of 15 deg and two sun azimuths of 90 and 45 deg, respectively

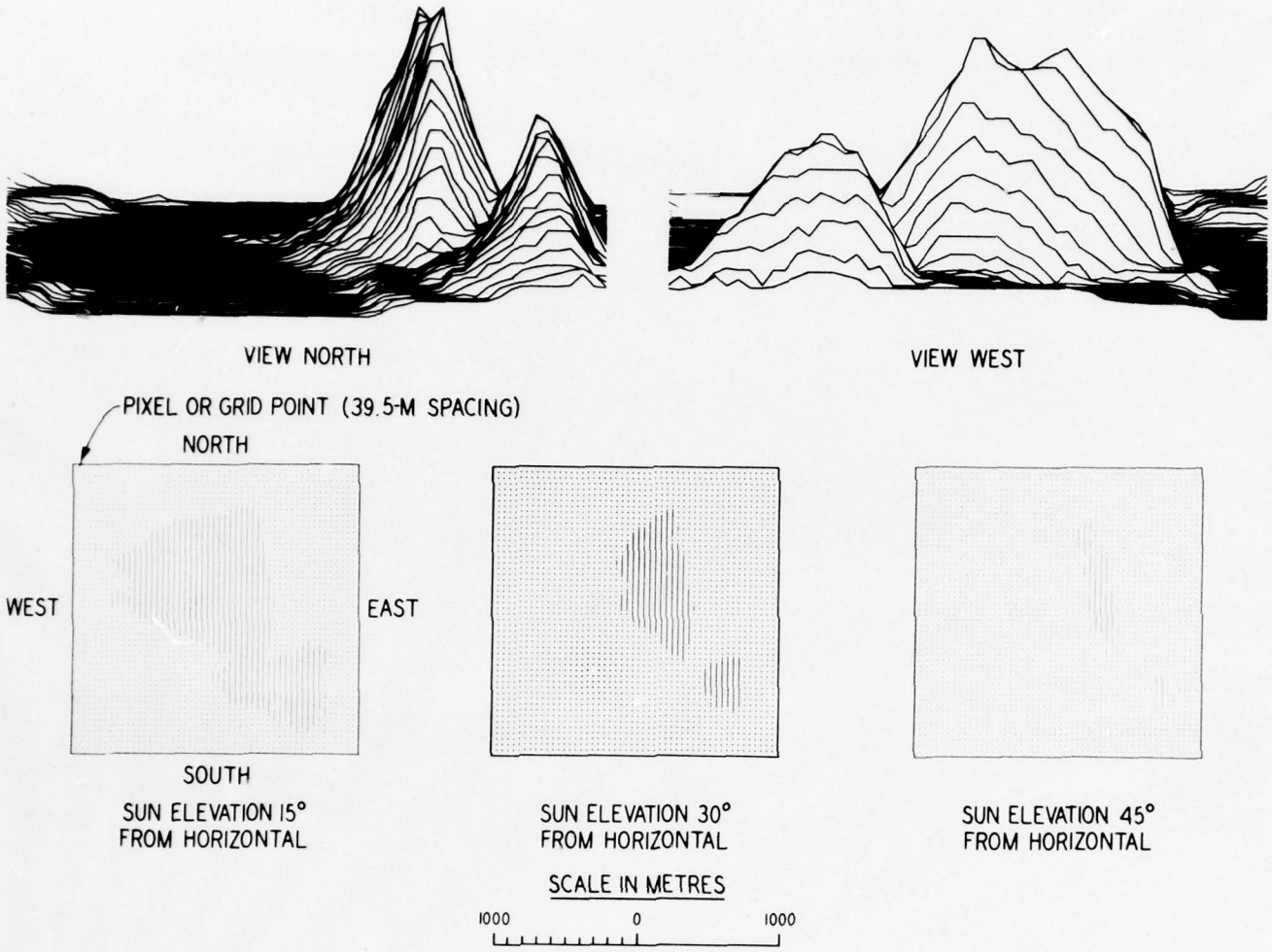

Figure 13. Ground area in shadow for a common sun azimuth of 90 deg and three sun elevation angles of 15, 30, and 45 deg, respectively

(Figure 13), the ground area in shadow became smaller as the sun elevation angle got larger. For the sun elevation angles of 15, 30, and 45 deg, the number of pixels were determined to be 642, 294, and 92, respectively.

Consolidated Equation for Extrinsic Effects

66. All of the extrinsic effects (atmospheric, reflectance geometry, and shadows) have been explicitly expressed in the preceding paragraphs. This means that all of the expressions can be linked into a single consolidated equation that will simultaneously accommodate all of the effects. The equation is

$$R(\lambda) = I_o(\lambda)\, T_i(\lambda,\phi_{sun})\, S(\alpha)\, \rho(\lambda)\, T_r(\lambda,\phi_{sat})\, H_{\alpha\beta sv} \qquad (7)$$

where

$R(\lambda)$ = radiance as a function of wavelength (λ) as measured by the Landsat sensor system, W $cm^{-2}\mu m^{-1}$

$I_o(\lambda)$ = the solar radiance as a function of wavelength above the atmosphere, W $cm^{-2}\mu m^{-1}$

$T_i(\lambda,\phi_{sun})$ = incident atmospheric transmittance coefficient as a function of wavelength (λ) and solar zenith angle (ϕ_{sun}), and represents the fraction of radiation transmitted through the atmosphere from the sun to the terrain surface, dimensionless

$S(\alpha)$ = slope attenuation coefficient for the effects of topography and sun position, dimensionless

$\rho(\lambda)$ = the reflectance signature (assuming a Lambertian surface) of the in situ terrain material with respect to the given wavelength λ, dimensionless

$T_r(\lambda,\phi_{sat})$ = reflected atmospheric transmittance coefficient as a function of wavelength (λ) and the satellite zenith angle (ϕ_{sat}), and represents the fraction of radiation transmitted through the atmosphere from terrain surface to the Landsat sensor, dimensionless

$H_{\alpha\beta sv}$ = the shadow coefficient, and a product of four functions H_α, H_β, H_s, and H_v, dimensionless

H_α = 1 if $\cos(\alpha) > 0$; angle α represents the angle between the sun position vector and the slope vector

$H_\alpha = 0$ if $\cos(\alpha) \leq 0$

$H_\beta = 1$ if $\cos(\beta) > 0$; angle β represents the angle between the satellite position vector and the slope vector

$H_\beta = 0$ if $\cos(\beta) \leq 0$

$H_s = 1$ if the terrain surface is determined not to be in a shadow

$H_s = 0$ if the terrain surface is in a shadow

$H_v = 1$ if the terrain surface is visible from the sensor (no obstruction between surface and sensor)

$H_v = 0$ if the terrain surface is obscured from the sensor (an obstruction exists between surface and sensor)

67. To obtain normalized radiance values (i.e. to remove the extrinsic effects from the measured radiance values), the equation is

$$||R(\lambda)|| = \frac{R(\lambda)}{I_o(\lambda)\ T_i(\lambda,\phi_{sun})\ S(\alpha)\ T_r(\lambda,\phi_{sat})} \qquad (8)$$

where

$||R(\lambda)|| = \rho(\lambda)$ = normalized radiance values

This equation makes it possible to convert the radiance values of images obtained at different times to a common datum.

PART III: POTENTIAL USES

68. As previously noted in Part I, the primary use for the extrinsic effects corrections will be in preprogrammed interpretation (or automatic interpretation). In brief, the corrections provide a way to "normalize" the radiance values, as recorded by the sensor, to the equivalent values at ground level. In theory, this provides a means of directly comparing field or laboratory measurements of terrain (or material)[7] radiance with the values at the sensor, whether in a satellite or aboard an aircraft.

69. The corrections also open the way to the solution of a somewhat more complex problem, namely change detection. Many of the practical engineering problems actually resolve into problems of change detection; for example, target detection. Modern camouflage is in many instances so good that an object, such as a vehicle or gun position, cannot be detected by examination of a single image; the carefully designed patterns on the camouflage materials blend nicely into the background. However, the patterns are <u>not</u> the same as in the original terrain. In principle, the change in actual pattern (<u>not</u>, be it noted, change in color or <u>type</u> of pattern) should be detectable by comparing before and after images. Thus, the problem becomes one of monitoring changes, i.e. change detection.

70. Similar problems are very common in the civil sector. Examples of these are detecting the beginnings of insect infestation in forests or agricultural areas, detecting illegal encroachments on waterways, small-scale changes in land use in urban areas, and so on almost without limit.

71. In concept, change detection is simple and straightforward. Let us assume two Landsat images, one taken in June and another in October of the year. Let us also assume that by some highly advanced technique it has been possible to bring the two images into perfect planimetric accord, so that there is a pixel-to-pixel match between the two images. At this point, there are two congruent data fields; each $\approx$ 57- by $\approx$ 79-m patch on the ground is represented by two sets of

radiance values. Obviously, the thing to do is to compare the radiance values set by set, and those pixels that exhibit a difference in one or more of the values indicate that the terrain conditions have changed between June and October.

72. The fact is that it does not necessarily mean any such thing. It is far more likely that the change is the product of one or more of the extrinsic effects. The seasonal character of the atmosphere has certainly changed. The haze condition may be different. Unless all of the laws of nature have been violated, the position of the sun in the sky will almost certainly be different. The consequence of all of these factors acting in concert is that, even if no actual changes occur on the ground, the record will indicate that virtually every pixel has changed, to at least some degree. The question is: Which are the "natural" changes, and which are the "artificial"?

73. Clearly, one approach to this problem is to "normalize" the radiance values to a common datum. In the example presented in paragraph 71, the procedure might be to bring the June radiance values to the values that would have been exhibited had the conditions (i.e. seasonally controlled atmospheric attenuation, haze, and solar zenith and azimuth angles) been the same in June as in October. Figures 6 and 10 are examples of the magnitudes of the corrections that are required. At this point, any differences in the value sets after correction can be ascribed to "real" changes on the ground.

74. In passing, and to belabor the obvious, the changes may not be due to anything "artificial." A spectral record of an oak forest in October in mid-latitudes in North America may well exhibit a spectrum rich in reds and yellows; whereas, the same forest in June will exhibit a spectrum rich in greens, with correspondingly reduced values of red. The spectral changes are evidence only of the normal seasonal responses of oak trees. This is, of course, the reason for Blocks 9 and 10 in Plate 1 in the "ideal" interpretation system. The predictive capability will presumably forecast the seasonal natural changes and thus provide a suitable standard of comparison. Thus, the "comparison" described in paragraphs 71 and 72 cannot be envisioned as one-to-one identities;

rather, the June values are compared with predicted June values, and the October values with predicted October values. The June image is used to define the distributions of terrain "types," and the October image is used to determine if there has been a change in those distributions.

PART IV: CONCLUSIONS AND PLANS

Comments and Conclusions

75. The symbolizations in Plate 1 indicate that all but one of the basic steps required by the "ideal" programmed interpretation have been solved, in the sense that computer programs exist that will perform the basic operations. This does not mean that there is in existence an "automatic interpretation" program. At the present state of development, the various programs exist as individual entities, and some have special constraints that make it impossible to use them except with data fields formatted in very special ways. Furthermore, little attention has yet been paid to linking the various programs into a single coherent system.

76. Consideration of Plate 1 will also reveal that the absolutely critical requirement for a mathematical model for predicting the radiance of terrain "types" is missing. Indeed, the work that has been done in this direction is extremely fragmentary, albeit quite extensive, as suggested by Reference 7.

77. It is also true that some of the existing programs are considerably less than ideal. For example, concepts exist that show promise of producing slope and aspect data much more elegantly and rapidly than is now possible. Since the production of slope and aspect maps is currently a relatively time-consuming and costly proposition, the new concepts should be explored. The primary reason for the high cost is the fact that digital elevation data are obtained from topographic maps by digitizing the contours on the map.[8]

78. It will not have escaped attention that no actual examples, in the form of processed images, of the effects of correcting for extrinsic factors have been presented in this report. It will also be noted that no field validations of the procedures have been conducted.

79. In summary, it may be concluded that:

a. Computer programs exist for handling all procedural requirements of the "ideal" programmed interpretation system except the radiance prediction model (Block 10, Plate 1).

b. The existing programs require modification to make them more general and to provide smooth linkages between them.

c. The existing programs and procedures should be validated with carefully designed field exercises.

Plans

80. Plans for the immediate future include the following:

a. Improving and linking the existing programs.

b. Designing and conducting a field validation exercise, including the preparation of sample products of all stages in the "ideal" procedure.

c. Initiation of the development of mathematical radiance prediction models.

REFERENCES

1. Struve, H. and West, H. W., "Acquisition of Terrain Information Using Landsat Multispectral Data; An Interactive Procedure for Classifying Terrain Types by Spectral Characteristics," Technical Report M-77-2, Report 2 (in preparation), U. S. Army Engineer Waterways Experiment Station, CE, Vicksburg, Miss.

2. Grabau, W. E., "Pixel Problems," Miscellaneous Paper M-76-9, May 1976, U. S. Army Engineer Waterways Experiment Station, CE, Vicksburg, Miss.

3. Link, L. E., Jr., "Procedures for the Systematic Evaluation of Remote Sensor Performance and Quantitative Mission Planning," Technical Report M-76-8, Aug 1976, U. S. Army Engineer Waterways Experiment Station, CE, Vicksburg, Miss.

4. Kennedy, J. G. and Williamson, A. N., "A Technique for Achieving Geometric Accordance of Landsat Digital Data," Miscellaneous Paper M-76-16, Jul 1976, U. S. Army Engineer Waterways Experiment Station, CE, Vicksburg, Miss.

5. Struve, H., "An Automated Procedure for Slope Map Construction," Technical Report M-77-3 (In 2 Vols), Jun 1977, U. S. Army Engineer Waterways Experiment Station, CE, Vicksburg, Miss.

6. Selby, J. E. A. and McClatchey, R. M., "Atmospheric Transmittance from 0.25 to 28.5 μm: Computer Code LOWTRAN 2," AFCRL-72-0745, Environmental Research Paper No. 427, 29 Dec 1972, U. S. Air Force Cambridge Research Laboratories, Bedford, Mass.

7. Longshaw, T. G., "Application of an Analytical Approach to Field Spectroscopy in Geological Remote Sensing," Modern Geology, Vol 5, 1976, Gordon & Breach, Science Publishers, Ltd., United Kingdom.

8. West, H. W., Doiron, P. L., and Parks, J. A., "Analytical Study of Ground-Surface Shielding Characteristics of Selected Road Terrains; Development of Shielding Model and Analyses of Results," Technical Report M-74-4, Vol I, Jun 1974, U. S. Army Engineer Waterways Experiment Station, CE, Vicksburg, Miss.

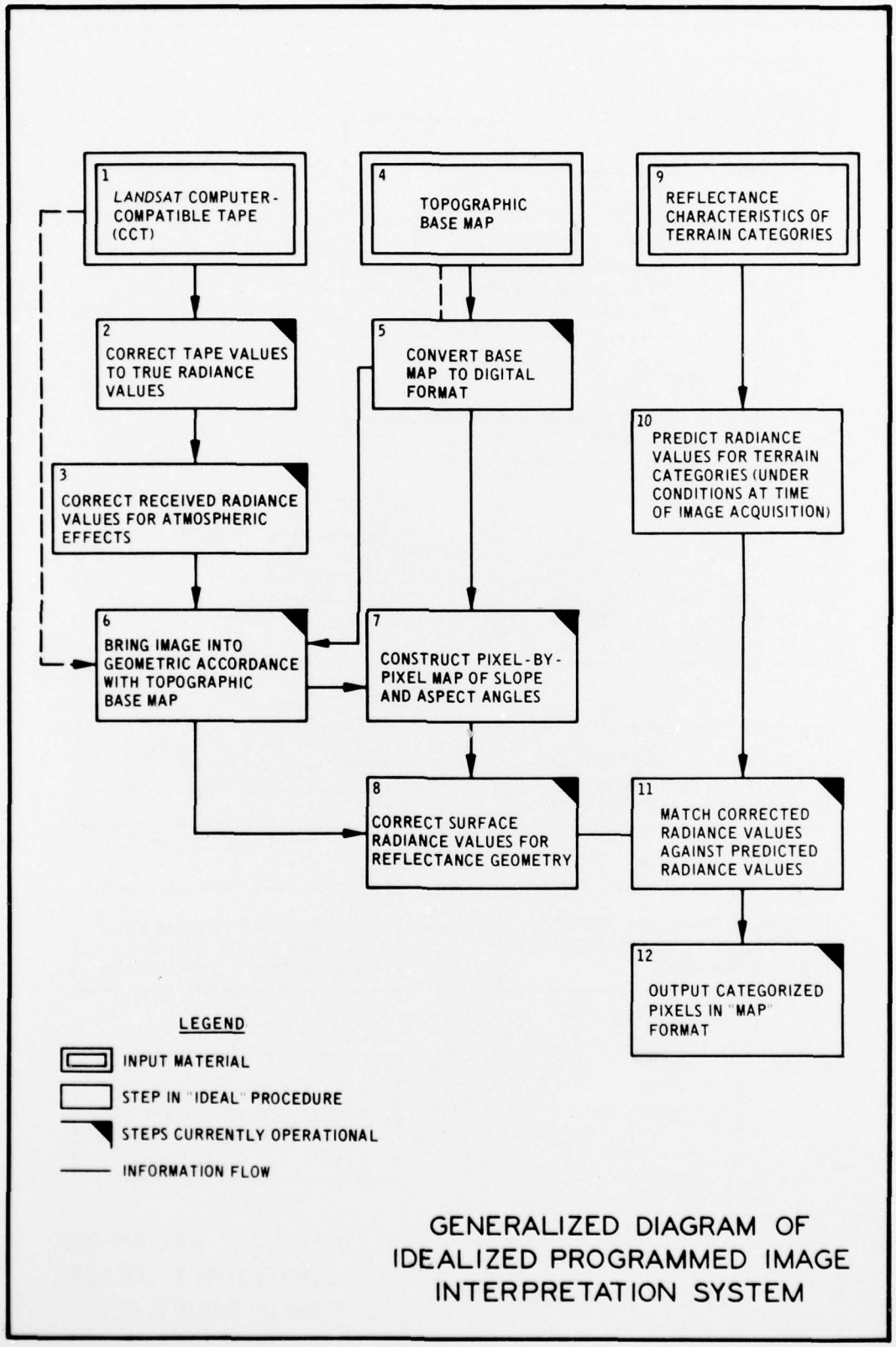

GENERALIZED DIAGRAM OF IDEALIZED PROGRAMMED IMAGE INTERPRETATION SYSTEM

PLATE 1

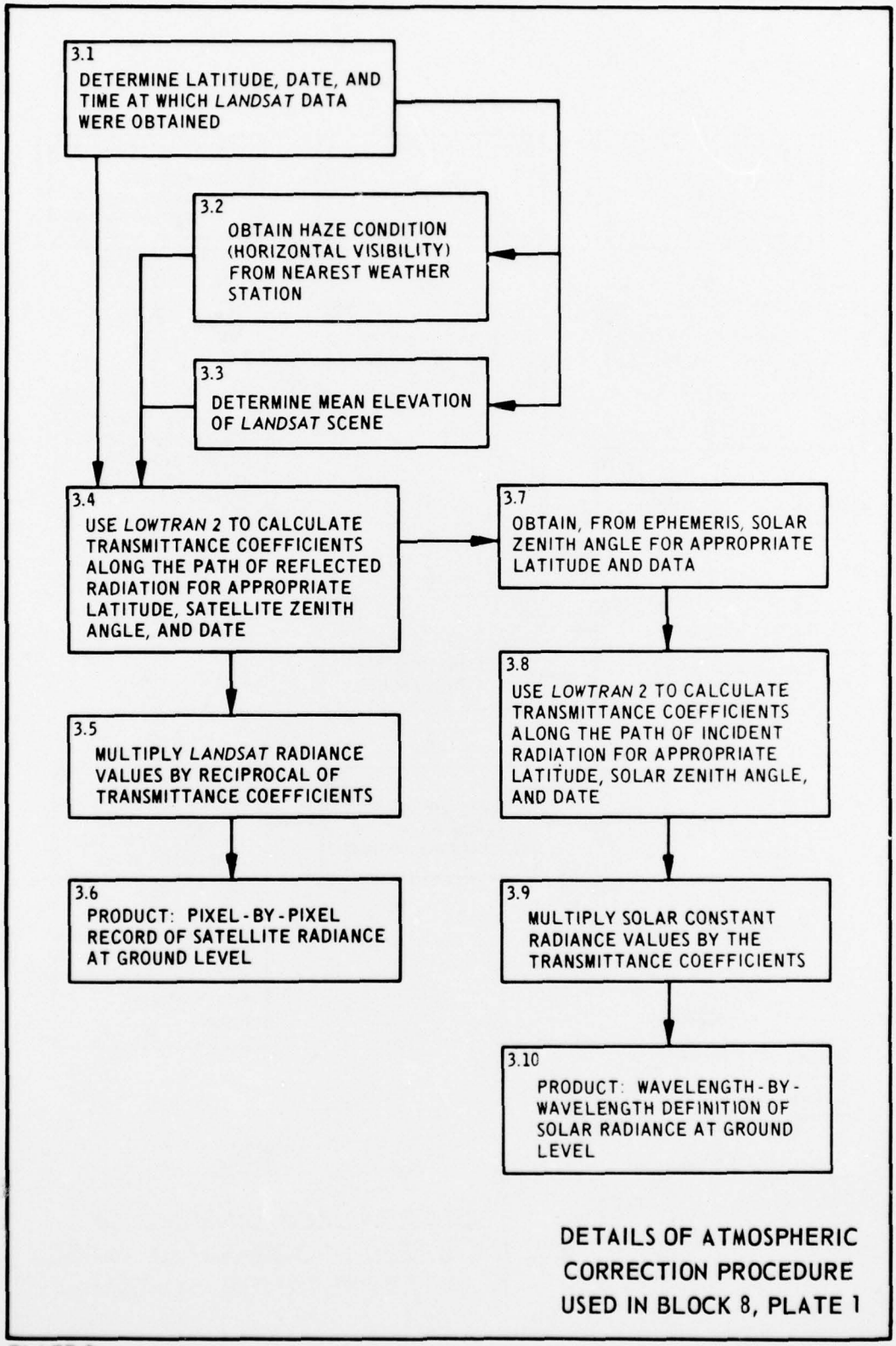

DETAILS OF ATMOSPHERIC CORRECTION PROCEDURE USED IN BLOCK 8, PLATE 1

PLATE 2

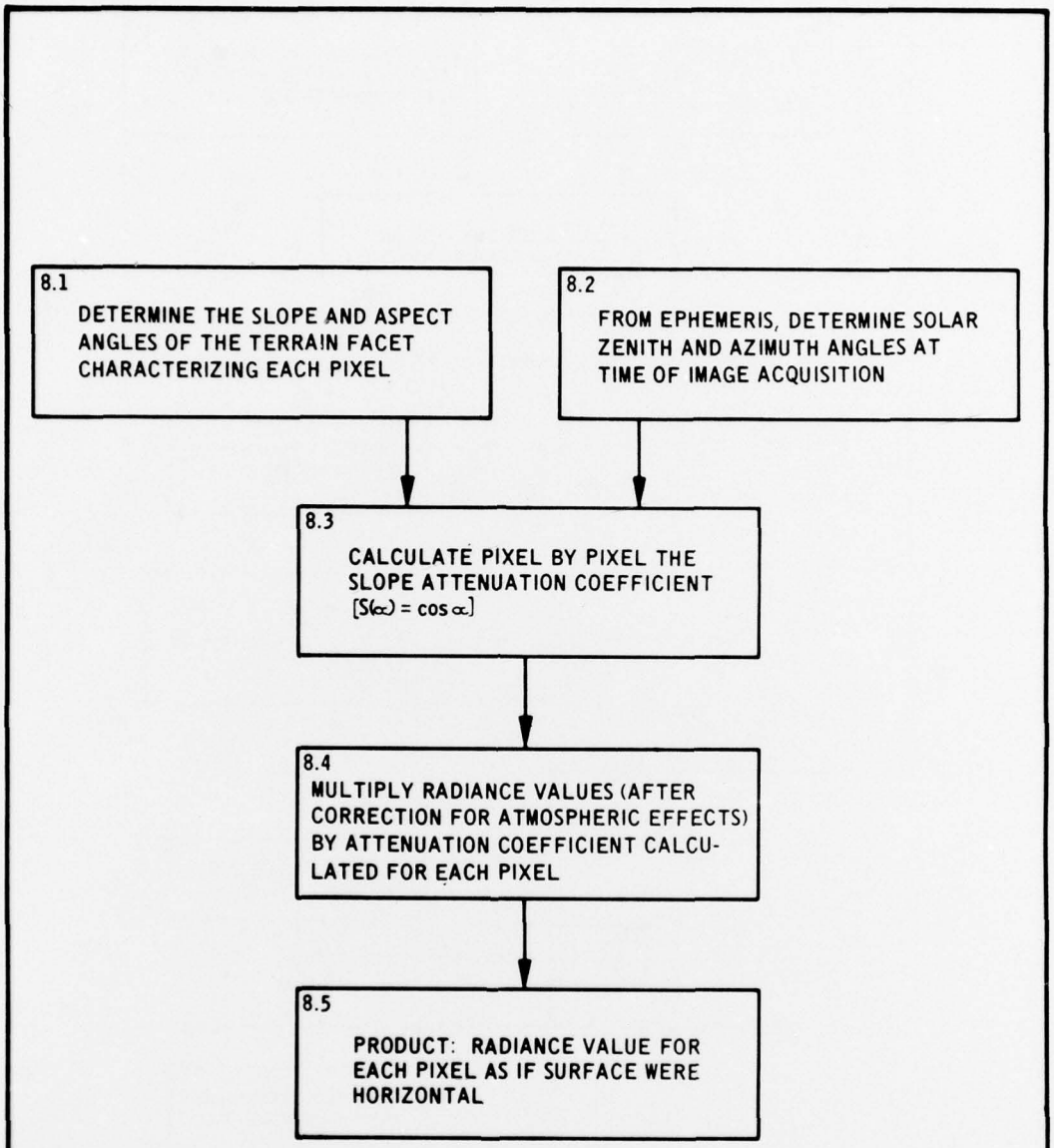

DETAILS OF SLOPE CORRECTION PROCEDURE USED IN BLOCK 8, PLATE 1

PLATE 3

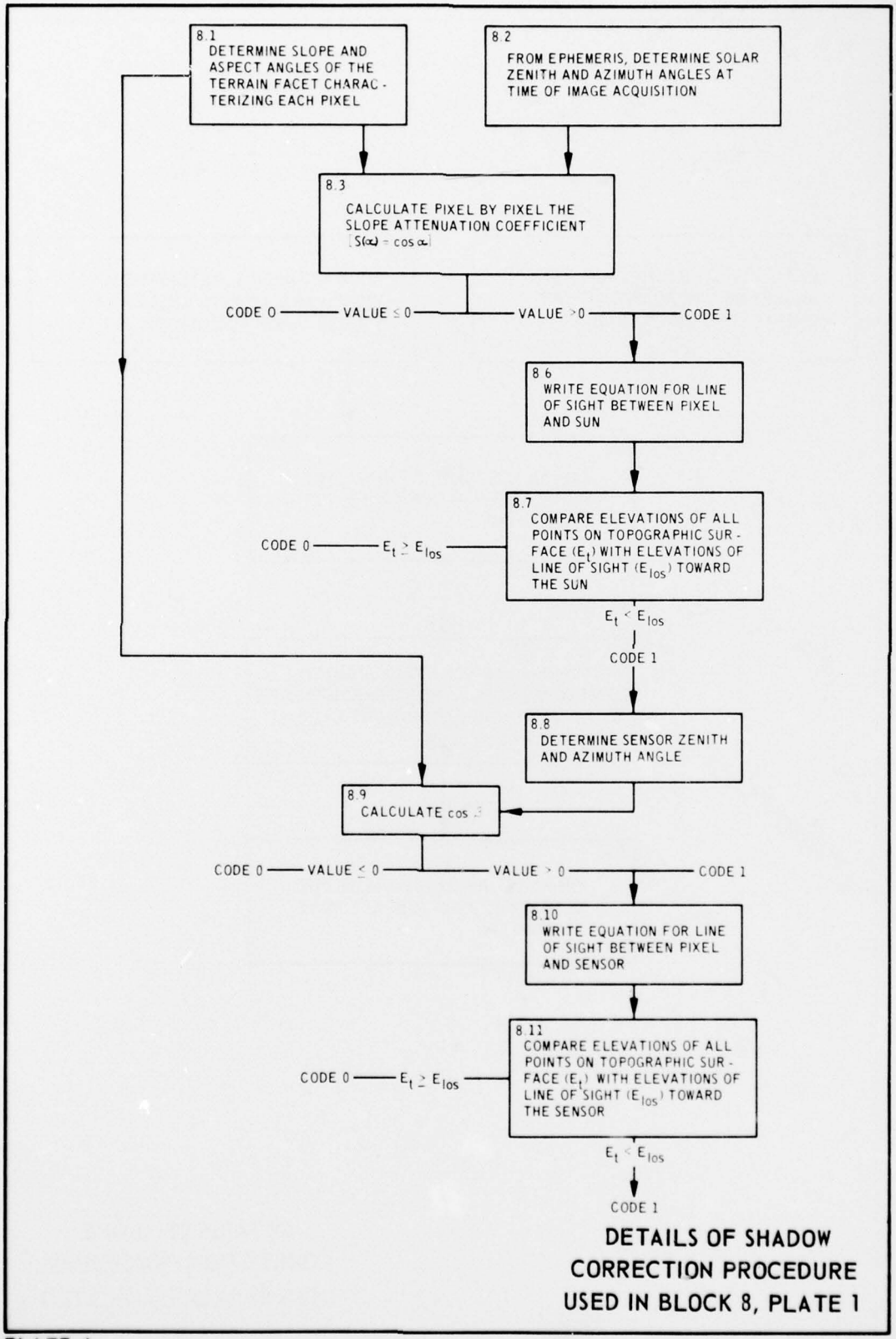

DETAILS OF SHADOW CORRECTION PROCEDURE USED IN BLOCK 8, PLATE 1

PLATE 4

In accordance with ER 70-2-3, paragraph 6c(1)(b), dated 15 February 1973, a facsimile catalog card in Library of Congress format is reproduced below.

Struve, Horton

Acquisition of terrain information using Landsat multispectral data; Report 1: Correction of Landsat multispectral data for extrinsic effects, by Horton Struve, Warren E. Grabau, [and] Harold W. West. Vicksburg, U. S. Army Engineer Waterways Experiment Station, 1977.

[59] p. illus. 27 cm. (U. S. Waterways Experiment Station. Technical report M-77-2, Report 1)

Prepared for Assistant Secretary of the Army (R&D), Department of the Army, Washington, D. C., under Project 4A061101A91D, Task 02, Work Unit 095 Q6.

References: p. 46.

1. Data acquisition. 2. Landsat (Satellite). 3. Multispectral data. 4. Remote sensing. 5. Terrain data. I. Grabau, Warren E., joint author. II. West, Harold W., joint author. III. U. S. Office of the Chief of Research and Development. (Series: U. S. Waterways Experiment Station, Vicksburg, Miss. Technical report M-77-2, Report 1)

TA7.W34 no.M-77-2 Report 1